UTRC88-38

(4)

AD-A198 917

ACCELERATED COMBUSTION THROUGH STREAMWISE VORITCITY STIRRING

John B. McVey

August 1988

UNITED TECHNOLOGIES RESEARCH CENTER

DTIC
ELECTE
SEP 0 2 1988
S   D
H

88 9 ... 0 ... 0

UTRC88-38

REPORT DOCUMENTATION PAGE

1a. REPORT SECURITY CLASSIFICATION			1b. RESTRICTIVE MARKINGS	
Unclassified				

2a. SECURITY CLASSIFICATION AUTHORITY	3. DISTRIBUTION / AVAILABILITY OF REPORT
2b. DECLASSIFICATION / DOWNGRADING SCHEDULE	Unlimited

4. PERFORMING ORGANIZATION REPORT NUMBER(S)	5. MONITORING ORGANIZATION REPORT NUMBER(S)
UTRC 88-38	

6a. NAME OF PERFORMING ORGANIZATION	6b. OFFICE SYMBOL (If applicable)	7a. NAME OF MONITORING ORGANIZATION
United Technologies Research Center		Office of the Chief of Naval Research

6c. ADDRESS (City, State, and ZIP Code)	7b. ADDRESS (City, State, and ZIP Code)
Silver Lane East Hartford, CT 06108	Arlington, VA 22217-5000

8a. NAME OF FUNDING / SPONSORING ORGANIZATION	8b. OFFICE SYMBOL (If applicable)	9. PROCUREMENT INSTRUMENT IDENTIFICATION NUMBER
		Contract N00014-86-C-0423

8c. ADDRESS (City, State, and ZIP Code)	10. SOURCE OF FUNDING NUMBERS			
	PROGRAM ELEMENT NO.	PROJECT NO.	TASK NO.	WORK UNIT ACCESSION NO. 4329-472

11. TITLE (Include Security Classification)

Accelerated Combustion Through Streamwise Vorticity Stirring   (U)

12. PERSONAL AUTHOR(S)   McVey, John B

13a. TYPE OF REPORT	13b. TIME COVERED	14. DATE OF REPORT (Year, Month, Day)	15. PAGE COUNT
Final Report	FROM 6/1/86 TO 6/30/88	1988 August 31	64

16. SUPPLEMENTARY NOTATION

17.	COSATI CODES		18. SUBJECT TERMS (Continue on reverse if necessary and identify by block number)
FIELD	GROUP	SUB-GROUP	Flame Propagation, Turbulent Combustion,
			Vorticity, Streamwise Vorticity,
			High-Speed Flow, Combustion,

19. ABSTRACT (Continue on reverse if necessary and identify by block number)

Experiments were conducted to observe the effect of streamwise vorticity on the rate of propagation of confined, high-speed, non-premixed turbulent flames. Water-flow visualization experiments were first conducted to establish the scale and intensity of the vortex arrays generated by convoluting the trailing edge of the splitter separating two parallel streams; one stream representing the oxidizer and the other stream representing the fuel. Combustion experiments then conducted; these experiments determined that the splitter plate design which generated the most intense vortex array in cold flow caused the flame spreading rate to be roughly twice that produced by a conventional flat splitter. Flame spreading rates were determined by photographing the direct flame emission radiated by atmospheric pressure flames. *Keyword*

20. DISTRIBUTION / AVAILABILITY OF ABSTRACT	21. ABSTRACT SECURITY CLASSIFICATION
☒ UNCLASSIFIED/UNLIMITED ☐ SAME AS RPT ☐ DTIC USERS	Unclassified
22a. NAME OF RESPONSIBLE INDIVIDUAL Gabriel D. Roy	22b. TELEPHONE (Include Area Code) (202) 696-4406 22c. OFFICE SYMBOL

UTRC 88-38

Accelerated Combustion Through

Streamwise Vorticity Stirring

ABSTRACT

Experiments were conducted to observe the effect of streamwise vorticity on the rate of propagation of confined, high-speed, non-premixed turbulent flames. Water-flow visualization experiments were first conducted to establish the scale and intensity of the vortex arrays generated by convoluting the trailing edge of the splitter separating two parallel streams; one stream representing the oxidizer and the other stream representing the fuel. Combustion experiments were then conducted; these experiments determined that the splitter plate design which generated the most intense vortex array in cold flow caused the flame spreading rate to be roughly twice that produced by a conventional flat splitter. Flame spreading rates were determined by photographing the direct flame emission radiated by atmospheric pressure flames.

ACKNOWLEDGEMENTS

DTIC
COPY
INSPECTED
1

Accession For

NTIS GRA&I	☑	
DTIC TAB	☐	
Unannounced	☐	
Justification		

By
Distribution/
Availability Codes
Avail and/or
Dist Special

A-1

i

UTRC 88-38

Accelerated Combustion Through Streamwise Vorticity Stirring

TABLE OF CONTENTS

LIST OF SYMBOLS

A	Flow area
B	Duct height
	Frequency
H	Lobe height
V	Velocity
W	Lobe width
x	Streamwise coordinate
α	Angle
ϕ	Equivalence ratio

Subscripts

p, pri	Primary stream (above the splitter plate)
s, sec	Secondary stream (below the splitter plate)

INTRODUCTION

The achievement of increased rates of flame propagation in confined, turbulent, high-speed streams has been a goal of combustion engineers since the introduction of jet propulsion engines. Classical experimental efforts (Williams et al. 1949, and Wright and Zukoski, 1962) to evaluate the influence of fuel-air ratio, approach flow turbulence level, pressure, and initial temperature on the spreading angle of confined flames have shown that the time-mean spreading angle varies only slightly in a range from 3-7 deg. These results, applicable to flames wherein the characteristic flow velocity is orders of magnitude higher than the burning velocity of the mixture (Bray and Libby, 1976), are consistent with a physical model (Spalding, 1967) in which the shear interaction between the differentially accelerated low-density combustion products and the high-density unburned gases acts to produce turbulence which controls the mixing rate; i.e., the shear-generated-turbulence effects dominate all other fluid mechanic phenomena. As a consequence, practical means of shortening combustion chambers have been limited to the use of multiple flame initiation sites (multiple bluff-body stabilizers) or the use of swirlers, both of which introduce a significant momentum loss in high-speed streams.

There is growing evidence that the introduction of arrays of streamwise vortices can have a dramatic effect on mixing-controlled flow phenomena. A large body of work performed on turbofan-engine forced mixers, which are employed to promote mixing of the hot, high-velocity core-engine exhaust stream with the colder, low-velocity fan air, has shown that under certain conditions extremely rapid mixing can be achieved. In a detailed examination of the velocity field produced by a forced mixer, Paterson (1984) showed that the rapid mixing is associated with the existence of intense, large-scale, streaming vortices. The sense of rotation of the vorticies alternates (Werle, Paterson and Presz, 1987) such that no net angular momentum is imparted to the flow. One method of generating such vortices is through the use of convoluted surfaces, Fig. 1. Based on flow-visualization evidence, the action of these vortices is first to cause a large-scale exchange of fluid (stirring) followed by a rapid breakdown of this organized structure into random turbulence. Importantly, measurements of the performance of mixer-nozzles (Skebe, Paterson and Barber, 1988) and ejectors (Presz, Gousy and Morin, 1986) in which this mixing concept has been employed, have shown that the increased mixing is accomplished without incurring significant momentum loss.

Because the processes of large-scale exchange followed by rapid breakdown to the fine scale are exactly what is desired in the high-speed combustion process, an experimental effort was conducted to determine if a significant increase in flame spreading rate could be observed if the flow were so preconditioned. The flow process has been termed "streamwise-vorticity-stirred combustion".

Streamwise vortex arrays can be generated using techniques other than the convoluted splitter plate. Bevilaqua (1973) showed that the rate of entrainment of an exhaust jet with the surrounding environment could be enhanced if the single jet were replaced with a series of adjacent jets which were canted at a small angle relative to one another. Streamwise vortices are

developed at the interface between jets. Rogers and Bendot (1976) reported on attempts to apply this concept to the combustion chamber of a ramjet engine; success was limited due to hardware problems. This scheme could only be applied in combustion situations where one stream (the jets) were at an initially higher total pressure than the other--such as a ducted rocket where the rocket chamber which delivers the fuel to the air stream can be at a high pressure. The essential difference between the use of canted jets and the use of convoluted mixer lobes lies in the high momentum loss associated with the use of canted jets. That is, when all of the jet flow is diverted at some angle; e.g. 15 deg relative to the flow direction, then a loss in streamwise momentum can be expected which will be on the order of the magnitude of the tangent of the cant angle. In the case of the convoluted surface, the evidence is that the vortices are formed in a much more efficient manner from the point of view of pressure loss.

In other related work, Gutmark, Schadow et al. (1987) have performed experiments in dump combustors wherein the entrance flow approaching the dump plane is passed through a duct which undergoes a transition from a circular cross-section to an elliptical or a slot-shaped cross-section. Flow visualization studies indicated that axially-aligned vortices were formed by the transition process. Combustion studies indicated the combustion rate was augmented.

The approach used in the program was to attempt to exploit the highly efficient means of generating vortex arrays offered by the convoluted splitter surface technique. Convoluted surface designs were selected which, based on prior experience, would generate an array of intense, large-scale streamwise vortices. Flow visualization studies were performed under isothermal conditions to establish that a streaming vortex array of suitable character was in fact generated; then combustion tests were performed to observe the flame spreading angle produced in a combusting flow.

CONVOLUTED SURFACE DESIGN

The physical processes important to the generation of streamwise vorticity by a convoluted surface are illustrated in Fig. 1. As the flow proceeds over the convoluted surface, the pressure field developed by the splitter contour and the geometry of the confining enclosure cause a deflection of the flow, directed from crest to trough, to develop. The important process is the inviscid effect of the pressure field. Although the flow in the boundary layer must undergo a greater degree of turning than the mainstream flow, there is no firm evidence that the boundary layer characteristics are important to the intensity and scale of the vortices generated.

The principal viscous effect is the departure of the flow from the surface at the trailing edge (the Kutta condition). This flow separation results in the development of regions of very high shear as the upward deflected flow from beneath the surface contacts the downward deflected flow from the upward surface. The corresponding vorticity which is developed is zero at the crest and trough of the lobe; maximum at midspan, and the sense of rotation alternates from one side of each lobe to the other.

Immediately downstream of the splitter trailing edge, vortex roll up occurs wherein the above-described vortex line develops into discrete, large-scale, streamwise vortices; each vortex is centered more or less at the location of maximum trailing edge vorticity. The formation of these discrete vortical flow structures is an inviscid effect and should be predictable by analysis of the inviscid, rotational flow.

The geometric parameters which affect the generation of vorticity by a convoluted surface are shown in Fig. 2. Although analytical methods are under development for treating the three-dimensional flow (Skebe, Paterson and Barber, 1988), the design approach used here was to apply experience regarding the range of the design parameter values which had proven to be effective in previous studies. A major factor influencing lobe design is the ratio of the flow rates in the two channels which the splitter divides. For the combustor application, it was desired to consider the case where a relatively small flow acts to pilot a larger flow. This results in an asymmetric lobe design (Fig. 3) where the smaller, secondary flow passes through a high aspect ratio channel while the larger primary flow passes through a low aspect ratio channel. The lobe penetration (lobe amplitude as a percentage of duct height) is limited by the maximum allowable aspect ratio. This maximum aspect ratio is determined by boundary layer build-up considerations. In the present case, the penetration (35%) was significantly less than prior experience dictated was required to ensure high mixing effectiveness and therefore the potential for achieving a high mixing rate was limited.

This compromise of reduced potential for achieving high mixing rate was accepted because of the overriding desire to maintain that characteristic which distinguishes a piloted flame--low pilot flow relative to mainstream flow. In fact, even lower penetration would be desirable in a combustor application because it should result in a lower momentum loss and a smaller surface area subject to thermal distress.

A second lobe design representing another extreme was also evaluated in this effort. This was a symmetric 2.54-cm amplitude lobe which was expected to produce streamwise vortex arrays, the development of which would be relatively free of any wall effects associated with the close proximity of the lower enclosure wall. Because of the small penetration (18%), it was not expected that large downstream influences would be observed, however, previous work performed with this lobe design indicated that local vortex arrays at the splitter trailing edge would be formed, and it was expected that some impact on combustion might be observed. A photograph of this lobe is given in Fig. 4.

FLOW VISUALIZATION TESTING

Test Apparatus

Flow visualization tests to verify the capability of the selected designs for producing streaming vortex arrays were conducted using water as the test

fluid and using gas bubbles and fluorescent dye as tracers. Water, as opposed to air, is used in flow visualization testing because approximate Reynolds number similarity is achieved at much lower velocities and therefore the flow patterns are easier to interpret and record. A schematic diagram showing the features of the apparatus is given in Fig. 5a; a photograph of the test apparatus is given in Fig. 5b.

Independently-controlled flows pass through the upper and lower channels of the facility. The flow through each channel is monitored by turbine meters. The range of flow rates obtainable through each channel and the corresponding flow velocity is given in Table 1. Note that for the most part, testing could be accomplished for conditions where the flow velocity through the lower channel was equal to or greater than the velocity in the larger upper channel.

Table 1 – Flow Visualization Facility Flow Capacity

| Upper Channel (Primary) | | | Lower Channel (Secondary) | | |
Meter Reading (CPS)	Flow Rate (l/s)	Velocity (m/s)	Meter Reading (CPS)	Flow Rate (l/s)	Velocity (m/s)
40	3.4	0.20	50	2.9	1.0
30	2.5	0.15	40	2.3	0.8
25	2.1	0.13	30	1.7	0.6
20	1.6	0.10	20	1.1	0.4
10	0.79	0.05	10	0.57	0.2

The gas bubbles used for visualization are formed in the fluid by accelerating the flow through an orifice such that the pressure is reduced to the point where the dissolved air comes out of solution. The bubbles formed are distributed fairly evenly throughout the flow and are of a sufficiently small diameter that the buoyancy effects are not significant given the flow times existing in the model. The dye used for visualization is a yellow fluorescein dye which fluoresces when illuminated by an argon-ion laser. The dye is injected from probes formed from 1.5 mm hypo tubes--the probes are manually positioned. Both 35mm still photography and video recordings are employed to record flow patterns of interest.

Test Configurations

The parameters specifying the splitter characteristics which were tested are listed in Table 2. The flow in the upper channel--the flow over the upper surface of the lobe--is referred to as the primary flow in this report; the lower channel flow is the secondary flow. In addition to the two lobes being installed in the conventional manner (with the lobe plan parallel to the floor of the channel), the 35% penetration lobe was tested with a ramp installed on the lower wall. The purpose of the ramp was to raise the lobe trailing edge from the vicinity of the lower wall such that the wall would not adversely effect the pressure field generated by the lobe/enclosure configuration. When the ramp was installed, the splitter surfaces were canted such that the flow

area under the ramp remained constant with streamwise distance whereas the area over the lobe underwent a slight contraction (Fig. 6). Also tested was a flat splitter, tapered to a trailing edge thickness (1.3 mm) approximating that of the material from which the lobes were manufactured; the flat splitter was tested both with and without the ramp. The configurations tested are shown schematically in Fig. 7.

Table 2 - Test Configurations

Splitter Configuration	Area Ratio	Lobe Amplitude (cm)	Lobe Aspect Ratio* (Pri/Sec)**	Profile Angles (deg) (Pri/Sec)
Flat Plate	6.96	0	0	0
Flat Plate w Ramp	5.74	0	0	0
18% Lobe	6.96	2.54	1.0/1.0	15/15
35% Lobe	6.96	4.9	1.7/4.6	15/7.4
35% Lobe w Ramp	5.74	4.9	1.7/4.6	15/7.4

* Aspect ratio is peak-to-peak amplitude divided by distance between lobes.
** Primary to secondary.

Test Results

a. Flat Plate

The flat plate tests served to establish a baseline for judging mixing rates. No unexpected flow trend was observed. The flow remained attached to the tapered splitter trailing edge as expected. Dye traces produced a plume which expanded at the rate associated with a jet in turbulent flow. For the range of flow velocity ratios tested, the rate of entrainment of the primary flow into the secondary flow was small.

b. 18% Penetration Lobe

The overall character of the flow was similar to that of the flat plate; no significant increase in the entrainment rate was observed. Efforts to examine the details of the flow at the lobe exit did show some indication of vortex development; but the effect was judged to be too small from the point of view of potential impact on combustion to warrant extensive investigation.

c. 35% Penetration Lobe

A large amount of testing was conducted with this configuration in order to uncover the existence of vortex arrays, but no significant vortical flow pattern was observed. By use of bubble streaks and a narrow sheet of light grazing the lobe trailing edge, it was possible to discern evidence of motion in the transverse directions; but as the light sheet was moved downstream the development of large scale vortices (roll-up) was not discernible. The use of dye jets indicated that there was some large-scale unsteadiness introduced

into the flow, but it was judged that the mixing between the streams was not significantly enhanced.

Extensive work was performed with dye probes located upstream of the trailing edge of the lobe in order to gain guidance as to how the lobe configuration might be modified in order to promote the development of the vortex array. If a higher penetration lobe were to be used, then there would be concern that the narrow passages through which the secondary stream flows would cause boundary layer effects to be dominant and the flow might separate from the lobe surface. No indication of flow separation was revealed by dye testing. Indeed, with the secondary flow velocity higher than the primary, some upward penetration of the lower flow was observed and this appeared to be the source of a random, large-scale unsteadiness observed in the downstream region. Tests performed using probes to inject dye on the upper surface revealed some evidence of the anticipated downward motion of the primary flow; it was apparent, however, that a stronger downward motion would be realized if the trough of the lobe were raised above the lower surface of the test section. It was this observation that led to the installation of the ramp, as described earlier.

d. Flat Plate with Ramp

This configuration served as a baseline with which to compare results obtained with lobe/ramp configurations. The separated flow region formed downstream of the step showed no unexpected behavior. The length of the recirculation region was approximately five step heights. Other than the displacement of the flow associated with the recirculation region, no change in flow character was apparent.

e. 35% Penetration Lobe with Ramp

Tests conducted with a sheet of light located immediately downstream of the trailing edge of the splitter provided dramatic evidence of the existence of intense, large scale vortices for this case. The evidence is made clear by the motion of the bubble tracers; some sense of this motion is conveyed by the streak photographs presented in Figs. 8 and 9. In Fig. 8, tracers are present in the upper stream. The short tracks in the uppermost portion of the flow are indicative of the relatively low transverse velocities in this region; the mean direction of motion is downward. It is significant that the vortices do, in fact, have an influence on the flow in a region removed from the immediate vicinity of the lobe surface. In the immediate region of the lobe, the very long streaks indicate the high-velocity vortical motion.

The paths of tracers introduced into the lower stream are illustrated in Fig. 9. The direction of movement is generally upward within the confines of the lobe surface. As the jet issues from the lobe, contact is made with the downward moving flow in the upper surface and a rapid turning to the downward direction occurs. The mushroom-like appearance of the tracers is characteristic of the pattern observed near the trailing edge of a lobed splitter when roll-up into discrete vortices occurs.

The severity and the large spatial extent of the flow turning which is associated with the presence of the vortex array is illustrated by dye traces (Fig. 10). The flow is from right to left; a dye probe is located just upstream of the field of view of the camera. The probe tip is in the midspan plane and is located approximately 2 cm below the upper wall. In the test, the velocity of the fluid beneath the lobe is approximately four times the velocity in the upper flow such that an ejector-like effect is produced. The entrainment of the low velocity fluid by the high-velocity fluid is so rapid that the fluid is actually torn away from the upper wall. The separated flow region is illustrated in Fig. 11 which shows the pattern obtained when injecting dye directly into separation bubble. The separation region downstream of the step is also made visible by dye entrained from a probe located in the lobe trough at the trailing edge.

In comparison to the baseline case of a flat plate splitter with the ramp, the recirculating flow behind the step exhibited less unsteadiness and the length of the recirculation zone appeared to be shorter--about two step heights. As noted before, the unusual separation on the upper wall was not evident in the baseline nor was the extent of entrainment of the upper flow worthy of note.

Observations of the existence of the vortices were made over the entire range of velocity ratios given in Table 1. Only when the lower flow was shut off, was the vortex motion not apparent.

COMBUSTION TESTS

Test Apparatus

A schematic diagram of the test apparatus used in the combustion program is given in Fig. 12. The cross-section is a 14-cm square. The apparatus is configured such that different splitter plate trailing edge geometries can be installed at a single, fixed height. The height of the splitter determines the area ratio between primary and secondary flow, and that area ratio is 7:1.

The apparatus is comprised of two sections: a preparation section in which the streams are conditioned and a combustion section equipped with two sets of windows through which the flame pattern can be observed. Both sections are uncooled; the combustion section is protected by a ceramic liner. The apparatus is rated for testing at atmospheric pressure. An overall view of the apparatus is provided in Fig. 13.

The trailing edge of the fixed position splitter is removable such that different lobe configurations can be attached. The total length of the splitter from the exit of the flow straighteners to the trailing edge of the lobe is 86 cm. The trailing edge of the splitter is located at the left-hand edge of a quartz window having a 12.7x28 cm viewing area. The total viewing distance (from the left edge of the left window to the right edge of the right window) is 65 cm. A close-up view of the test section with the high penetration lobe and ramp installed is given in Fig. 14.

The test apparatus was configurated to permit examination of the two classical flame types: premixed and non-premixed ("diffusion") flames. When testing in high speed flows, it is necessary to provide a mechanism for stabilizing the flame. In general, it is possible to heat the secondary stream (e.g. by partial combustion of the fuel) so that it acts as a hot gas pilot. In this case, to avoid the necessity of employing actively-cooled hardware, a mixture of pyrophoric fuel and nitrogen was used as the pilot stream. The pyrophoric fuel used was triethylborane (Appendix I) which has a reasonably short ignition delay time and which, being pyrophoric, ignites spontaneously in the presence of oxygen. In most tests, the nitrogen was heated to a temperature of 500K such that the liquid triethylborane would readily vaporize when injected. The TEB delivery system is visible at the left of Fig. 13.

For testing in the non-premixed mode, all of the fuel in the form of triethylborane is injected into the secondary stream. In the case of the premixed flame, only an amount of triethylborane sufficient to ignite the mixture is injected into the secondary stream, the balance of the fuel in the form of propane or Jet-A is injected far upstream of the test section entrance.

Further information on the test apparatus is contained in Appendix II.

Instrumentation and Control

Conventional instrumentation including venturis, turbine meters, mass flow meters, pressure gauges and thermocouples are used to monitor and control the state of the air (primary stream), nitrogen (secondary stream) and fuel flows. The extent of flame spreading is determined from direct flame emission photography. In this program, flame patterns were recorded using an autowinding 35 mm camera equipped with a 60 mm focal-length lens. ASA 400 color slide film was generally used in combination with a shutter speed of 1/60th sec. The framing rate was approximately 2 1/2 frames per second. A Locam high-speed motion picture camera operating at 100 frames-per-sec was also employed. The camera was equipped with an 18 mm focal length, f1.8 lens; ASA 400 film was used.

Additional instrumentation was employed for diagnostic purposes and control. A high frequency pressure transducer (Appendix III) was used to examine the nature of pressure oscillations which developed; the transducer output was digitized and recorded by the facility data acquisition system. Also, 3.2 mm-dia sheathed chromel-alumel thermocouples were inserted in instrumentation ports located on the top wall of the test section in order to detect the presence of combustion. Initially, these thermocouples were used to detect autoignition in the preparation section. Subsequently, this instrumentation was used to detect the flame boundary and specifically to establish that the observed flame patterns extended through the depth of the flow and were not merely a wall effect. The instrumentation ports were located on the test section roof, 3.8 cm on both sides of the center plane of the 14 cm-wide duct.

Control of the apparatus was accomplished through a combination of automated and manual systems. A microcomputer-based automated system was employed to ensure that events occurred in the proper sequence; e.g., the flow of pyrophoric fuel could not be initiated unless there was an appropriate flow of both primary and secondary gases. The flow levels were controlled manually. In virtually all cases, the flow levels were established prior to initiation of pyrophoric fuel flow. During the actual combustion run, it was necessary only to activate the recording equipment. A typical run duration was 20 seconds. Further details of the system are included in Appendix II.

Test Conditions

The primary parameters which were varied in the experimental program were the splitter plate lobe design, the velocities of the two streams, and the TEB flow rate. For all of the tests reported here, the apparatus was operated in the diffusion flame mode with all of the fuel being introduced as TEB. The equivalence ratio of the mixture was therefore determined by the TEB and air flow rates. No effect of stream temperature variation was observed during shakedown tests; therefore no systematic stream temperature variation was employed during data acquisition.

The range of test conditions covered is given in Table 3. The nature of the test effort was that of an exploratory effort to search for the existence of a phenomena; there was no intent to formalize a test matrix.

Table 3 - TEST CONDITIONS - Combustion Tests

Splitter Configuration	Primary Velocity (m/s)	Velocity Ratio	Equivalence Ratio	No. of Tests
Flat Plate	26.8 to 45.7	0.7 to 4.6	0.16 to 0.46	8
Flat Plate with Ramp	26.8 to 61.0	0.7 to 3.0	0.24 to 0.45	12
18% Penetration Lobe	26.8	1.5 to 4.6	0.16	5
35% Penetration Lobe	45.7	3.0 to 4.6	0.16 to 0.36	9
35% Penetration Lobe with Ramp	19.3 to 76.2	0.7 to 5.0	0.13 to 0.54	44

Primary Stream Temperature: 283 to 294 deg K
Secondary Stream Temperature: 528 to 639 deg K

Test Procedures

A test was conducted using the following procedure:

o The flow rate of the stream to be heated (usually the secondary nitrogen) was established; the electrical heater was energized; and a

period of time, several minutes, was allowed to elapse in order to stabilize the inlet temperature.

o The TEB cylinder pressure was preset to the desired level.

o The flow rate of the unheated stream was established.

o The video system was activated (including audio recording of all test conditions and observations).

o The automatic run control system was activated (TEB flow was initiated and combustion occurred); recording of thermocouple output was begun.

o The flame pattern was observed; if combustion was satisfactory, the run was continued.

o The 35-mm camera; the high-speed motion picture camera; and the high-speed data system for recording rig pressure fluctuations were activated. Generally, the 35-mm camera captured seven to ten frames, the motion picture camera recorded for five seconds and the high-frequency pressure transducer output was recorded for five seconds.

o The run control was commanded to shut the system down.

Test Results

Testing was carried out in two phases: 1) a survey to establish the operating characteristics of the apparatus and to select appropriate test conditions; 2) tests to evaluate the effect of streamwise vorticity stirring on flame propagation.

A summary of the results of the former test series is as follows:

o The TEB did serve the dual purpose of providing an ignition source and a heat source, but some undesirable characteristics were present.

    o A significant lag in the formation of a luminous flame was observed. An inspection of flame photographs showed that a pale blue flame existed at the moment of contact between the streams, but high-luminosity emission began significantly downstream of the splitter trailing edge. The camera aperture setting was dictated by the high luminosity flame, therefore the location of the flame at the splitter exit could not be recorded. As the primary stream velocity was increased, the luminous flame moved farther downstream. Increasing the primary stream temperature from 260 K to 533 K had no apparent effect on the location of the luminous flame.

    o The oxidation of the TEB produced boric oxide which stained the windows. The stain pattern developed immediately downstream of the trailing edge--in the "blue-flame" region. No attempt was

made to provide a window purge flow. The rate of deposition of oxide was sufficient to preclude the possibility using schlieren photography or any form of laser diagnostics.

o Injection of TEB at a location immediately upstream of the entrance to the preparation section produced rough combustion; evidence of droplet burning was recorded by the video camera. As a result, the TEB injection point was moved to a far upstream location and the nitrogen stream into which the TEB was injected was heated to approximately 500 K.

o Addition of Jet-A to the TEB/nitrogen stream had no apparent effect on the flame structure. Because it was simpler to operate the apparatus with a single fuel supply, all diffusion-flame testing was performed using TEB as the solitary energy source.

o Incomplete combustion of TEB produced a malodorous exhaust stream. Although not toxic in the concentrations present, the odor level in the water-deluge-scrubbed combustion products was highly objectionable.

o A steady and stable flame was achieved under a limited range of conditions. Unsteady flames or rough combustion were generally associated with operation at too-lean a mixture or too-high a velocity; i.e., conditions associated with the approach to a flammability limit. The identification of a rough combustion condition was easily performed by inspection of the video images at the time of testing. A second form of transient behavior, pulsating flames, existed at high fuel flows and at low stream velocities. The fact that a periodic combustion instability was excited was not unexpected; for purposes of this program it was possible to operate in a regime where the amplitude of the instability was not significant. The existence of the instability could not be detected by the video system because the frequencies (fundamental frequency of 30 Hz) were too high to be resolved. The flame patterns captured by the film cameras readily revealed the existence of the instabilities; and the results of these tests were not emphasized in the data analysis.

o Operation of the system in the premixed mode was briefly attempted, but positive results were not achieved due to facility problems. It had been anticipated that a program would be conducted using the premixed mode in order to minimize the consumption of the costly TEB. However, it became apparent that testing in the diffusion flame mode could be completed in a time period significantly shorter than that required to (manually) ramp the main fuel from zero (to avoid "hard starts") to full flow and thus TEB consumption would be minimized by testing in the non-premixed mode. As a consequence, all results reported are for the case of non-premixed combustion.

The results of the tests to document the extent of flame spreading achieved with the different lobe geometries and different flow conditions are

presented as photographs of the various flame envelopes. Typical photographs for each of the five configuration tests are presented herein as plates. The general view of the test apparatus captured by the 35 mm camera is shown as Plate 1. Generally, as noted above, the exposure time employed in capturing the flame envelope was not sufficient to permit the outline of the test apparatus to be totally resolved; this photograph provides a reference view. The figure also shows the location of the thermocouples which were used to provide verification of heat release in certain tests. The circular object behind the upstream window is a covered mirror employed in a schlieren system (not used in this program).

The flame produced by the flat splitter is shown in Plate 2. The typical characteristic of bright flame in the downstream window and the apparent existence of significant ignition delay is evident. Also evident is the film of boric oxide which readily formed on the windows. The oxide deposits did not present a problem in locating the flame front except in the region immediately downstream of the splitter trailing edge. Here, the background flame radiation is weak and is primarily in the blue spectrum to which the film is relatively insensitive. Consequently, the apparent envelope of the pale flame in the upstream region is, in fact, radiation which is scattered from the bright downstream flame by the oxide film. Wall effects played a role as to where the oxide was deposited, and hence there is not a one-to-one correspondence between the oxide film envelope and the flame envelope. This was apparent because the height of the oxide film at the splitter trailing edge was greater than the height of the splitter--some small leakage past the splitter plate edge immediately upstream of the trailing edge was the cause.

An example of existence of rough combustion is given in Plate 3; the leading edge of the flame front is highly distorted. Sequential frames on the film roll would exhibit a distinct lack of repeatability. Note that illumination of the boric oxide film by the downstream flame is quite evident in this photograph.

The envelope produced when the ramp was placed under the flat splitter is shown in Plate 4. Note that the thermocouples have been lowered into the flame front in this case.

Plates 5 and 6 show the envelopes obtained with the 18% penetration and 35% penetration lobes (with no ramp). Note the slight distortion of the flame envelope near the leading edge in Plate 6--evidence of rough combustion. The peculiar oxide coating pattern in the upstream region was the result of having flushed the test apparatus with fuel; liquid fuel was deposited on the window and washed away some of the oxide.

The flame pattern produced by the 35% penetration lobe and ramp is illustrated in Plate 7. In addition to the evident wider spreading angle, the flame intensity radiation is more brilliant and generally extends farther upstream.

To quantify these and other flame photograph results, the images recorded by 35 mm slide film were projected on a screen and the flame envelope traced. The tracing was digitized and the area under the flame envelope was

calculated. The digitized recordings for the photographs presented in the plates are given in Fig. 15; additional results are presented in Appendix IV. No attempt was made to match the height of the digitized flame at the splitter trailing edge with the height of the splitter. The error, associated with the obscuration of the flame by the oxide film, is especially apparent in the case of the flat plate splitter. The results for all of the cases in which the calculation were carried out are shown in Table 5.

Table 5 - Flame Envelope Evaluation

Configuration	Test	V_{pri} (m/s)	V_{pri}/V_{sec}	Equivalence Ratio, 0	Percent Coverage
Flat Plate	37	45.7	4.6	0.16	38
	49	45.7	4.6	0.16	46
	103	45.7	1.0	0.31	42
	104	38.1	0.83	0.35	43
Flat Plate with Ramp	120	30.3	0.7	0.43	52
	123	45.7	3.0	0.30	54
	125	45.7	1.5	0.31	51
	128	61.0	2.0	0.24	51
18% Penetration Lobe	52	45.7	4.6	0.16	59
	53	45.7	3.0	0.16	60
	55	45.7	2.0	0.16	59
35% Penetration Lobe	56	45.7	4.4	0.16	62
	61	45.7	4.6	0.16	65
	62	45.7	4.6	0.14	69
35% Penetration Lobe with Ramp	88	26.8	1.2	0.31	90
	91	38.1	0.83	0.36	90
	136	61.0	2.0	0.20	78
	137	45.7	3.0	0.25	84

The area under the flame envelope is expressed as a percentage of the total viewing area and is termed the "coverage". It is apparent that the calculated coverage values cluster about certain levels for each splitter configuration, the flat plate being the lowest and the high penetration lobe with ramp being the highest. Neither the velocity level, the velocity ratio, nor the equivalence ratio were observed to have a significant impact on coverage. Likewise, during the shakedown testing, stream temperature was not observed to have an effect. The only observed effect resulting from changes in the flow parameters was the nature of the combustion process—whether rough or smooth combustion occurred. The extent of flame spreading was controlled by the geometric nature of the splitter and duct.

Very high amplitude pressure oscillations occurred when testing the 35% lobe plus ramp configuration at equivalence ratios of 0.3 and above. The

regularity of the oscillations is revealed by the pressure transducer output and the results of a spectral analysis (Fig. 16). The images recorded by the high speed motion picture camera during unsteady operation showed that the flame front position varied to the extent that the flame totally disappeared from view and then totally filled both viewing ports. On the other hand, when the flat plate with ramp was evaluated under the same conditions, relatively smooth combustion occurred up to the highest equivalence ratio tested. The amplitude of the pressure oscillations was orders of magnitude lower and no dominant frequency was apparent (Fig. 17).

Because of the combustion instability which occurred when testing the 35%-lobe-plus-ramp configuration, considerable effort was expended to determine if there was a combination of flow velocity ratio and absolute velocity level where the magnitude of the flame oscillation was small when testing at high equivalence ratio. The highest equivalence ratio at which reasonably steady flow was achieved was 0.25. The flame image recorded is given in Plate 7; no detectable variation in the flame envelope is observed in the high speed motion pictures of that test.

The thermocouples which were extended into the flame zone from the upper wall were intended merely to provide evidence of the existence of a flame and not as a primary data source; however, the output does provide information of interest. The installation of the thermocouples was fixed as Configuration A (Fig. 18) for most of the tests; the thermocouple having the lesser immersion (T2) was further withdrawn (Configurations B and C) for a few tests. As indicated in the figure, Thermocouple T1 was extended to within 1.8 cm of the floor of the test section; this is the height of the edge of the trailing edge of the flat plate splitter in the case where no ramp was used. It was anticipated that for all cases where combustion occurred, this thermocouple would respond. Thermocouple T2 was extended a little more than halfway through the duct; this thermocouple was not expected to respond unless rapid flame propagation occurred.

The thermocouples were standard grounded thermocouples housed in a relatively large diameter (3.2 mm) stainless steel sheath; the response time was sufficiently slow such that under the test conditions, the test would be completed before burnout occurred. No attempt was made to measure actual flame temperature.

Thermocouple outputs obtained in tests conducted with the flat-plate-plus-ramp are shown in Fig. 19. The upper left figure (Test 120) presents the data corresponding to the flame photograph of Plate 4. The deeply immersed thermocouple (T1) shows a strong response whereas T2 shows no response. Inspection of Plate 4 shows the tip of that thermocouple to be immediately adjacent to the flame envelope; any slight improvement in flame spreading due to a favorable change in test parameters should cause T2 to respond. Note also the initial levels of temperature: Thermocouple T1 is located within the mixing region and the indicated level (375K) should lie between 533 and 290 deg K, the nominal temperatures of the two streams. On the other hand T2 is located outside of the mixing region, and the indicated level reflects the temperature of the air stream alone.

The upper right figure (Test 121) exhibits similar characteristics but shows a leveling off of T2 in the neighborhood of 750K. This characteristic was not usually observed. The equilibrium temperature for the overall combination of air, TEB, and nitrogen is approximately 1400K (Appendix I) and the local equivalence ratio would be even higher at the edge of the mixing layer. Generally, the indicated temperatures showed a continuous increase until run completion when both fuel flow and data recording were simultaneously terminated.

The lower left figure (Test 123) shows the results for a velocity ratio of 3 as opposed to the velocity ratio of 0.7 for the upper left figure. Note that T2 again has not responded--the change in velocity ratio did not cause the flame front to move over the tip of T2. The more rapid rise in T1 is associated with the lower level of nitrogen diluent and thus higher flame temperature.

The lower right figure (Test 128) shows the results for the highest velocity of primary flow tested. Indeed, for these tests and all eleven tests conducted in the series using the flat plate plus ramp, the response curves never indicated that the flame reached the height of the tip of Thermocouple T2.

The results obtained when employing the 35% lobe plus ramp are shown in Fig. 20. The upper left figure shows the results for Test 137 which corresponds to the flame envelope of Plate 7. Two points are important: (1) the thermocouple T2 has responded; (2) the initial level of temperature recorded by the two thermocouples is nearly identical. These features were present in all results obtained with this splitter configuration and thermocouple location. The response of T2 supports the visual observation that flame spreading was increased. The identical temperatures at the start of the run time reflects the fact that the lobe mixer has effectively mixed the two streams at this station over at least the vertical distance represented by the thermocouple spacing.

Results obtained with this configuration also lends support the belief that the observed flame envelope is representative of the state of the gas through the depth of the flow. The upper right figure (Test 134) shows results obtained under conditions in which a periodic oscillation occurred--the flame front was observed to oscillate fore and aft sweeping past the thermocouple station. The time-mean temperature recorded by thermocouples located 3.8 cm from on either side of the centerline of the 14-cm duct responded identically as would be the case if the flame front totally filled the duct as opposed to being merely a side-wall effect.

The responses obtained with Thermocouple T2 withdrawn by different degrees are given in the lower figures. In Test 142 the probe extended only 37% of the distance across the duct and a response was still obtained. A further withdrawal to 20% immersion (Test 144) produced no response from the thermocouple. Note, however, that the initial temperatures recorded by the thermocouples again indicate very effective mixing at this point.

DISCUSSION OF RESULTS

The cold flow visualization results indicated that intense large-scale vortices can be formed using convoluted surfaces having design characteristics suitable for mixing two flows of greatly differing flow rates. The previous work performed with this mixing concept (discussed in the Introduction) dealt primarily with streams with more nearly equal flow areas. These experiments were performed for flow in a duct wherein there is a 7:1 area ratio existed between the streams. This large flow ratio situation is characteristic of a high through-flow combustion device where a relatively small piloting stream is to initiate a propagating, turbulent flame.

The results showed that characteristics other than the lobe design were important to the existence of an intense vortex array--the geometry of the duct (the presence of the ramp) was crucial to the establishment of the vortex array.

The question remains as to whether there is a critical flow situation which must exist for the vortex array to develop. In these tests, two configurations were tested using the high penetration lobe. In the case where no ramp was employed on the floor of the test section, the observed magnitude of the flow rotation was exceedingly small. When the ramp was employed, the change in the flow field was dramatic; existence of an array of intense vortices was clearly evident. If experiments were conducted with a series of different ramp heights, then it would be possible to determine whether there is a continuous increase in local vorticity or whether there is a sudden increase. There has been some analytical work performed which suggests that the vortex roll-up process is a process that is "triggered" by certain flow conditions, but this analytical approach has yet to be fully explored. Given a flow geometry in which the roll-up does occur, the cold-flow visualization results indicated the existence of the roll-up was not sensitive to the velocity ratio of the streams. Nor was it necessary to tailor the character of the boundary layer flow on either side of the convoluted surface; nor was it necessary to tailor the free stream turbulence level. In this sense, the vortex development process was "robust".

The dominant features of the vortex array observed in the flow visualization tests were the intensity and scale of the vortices. The scale was on the order of the lobe height. The folding of one flow into the other resembled the motion induced by an egg-beater. The rotational velocity at the center of the vortices appeared to be very high.

The combustion test results indicate that the lobe surface and duct enclosure which produced intense vortices in cold flow had a dramatic effect on the flame propagation rate. The dilation effect associated with the heat release apparently did not destroy the flow structure which had previously been demonstrated to be effective in mixing non-exothermic flows.

There was no evidence uncovered which would suggest that the process would not be effective in even more energetic flows. (The extent of heat release achieved in these tests was less than originally planned because of the combustion instability which was excited at higher heat release.

Modifications to the test apparatus to alter the acoustic behavior were beyond the scope of this exploratory effort.)

The flame photographs can be interpreted in terms of a flame spreading angle. A measure of angle that is used by combustion engineers is defined by the lateral spread of the flame from the edge of the flame origin (e.g. V-gutter flameholder lip) to the combustor wall or the merge point with the adjacent flame and the associated distance from stabilizer to merge points. This definition is applied here except that the origin edge is taken to be the top of the slot through which the secondary flow would be passed if the splitter were not contorted by the convolutes. Because the flow area under the convolutes was constant, this position is, in fact, the position of the tip of the trailing edge of the flat plate. This position was at the left edge of the left window of the test section at a height which differed among the configurations only because of the presence of the ramp (Fig. 21). Using the digitized flame envelopes (Appendix IV), the slope of the line from this origin to intersection of the flame envelope with the right edge of the right window defined the spreading angle. For the two cases of the 35% lobe with ramp, where the flame appeared to fill the downstream window, the merge point was taken as the midstation of the window. The angles so determined are given in Fig. 22 where it is seen that the flame spreading angle associated with the 35% lobe with ramp is roughly double that of the flat plate.

The fact that the 18% lobe created an apparent flame spreading angle increase of almost 50% is unexpected in view of the lack of intensity of the vortices which were observed in the cold flow tests. There was some evidence of those tests of the creation of the vortex array in both this and the 35% lobe case (no ramp), but the motion was insufficient to justify much hot flow testing. A more extensive effort would have to be undertaken to verify the observation that the small penetration lobe could have a significant effect.

A legitimate question that is raised in conjunction with the reports of large increases in mixing associated with lobed mixers is whether the effect is merely the result of the increased wetted perimeter between the mixing streams or whether it is the result of streamwise vorticity stirring. In the present experiments, the ratio of the wetted perimeter of the 35% penetration lobe to the straight splitter is 1.9:1; for the 18% lobe the ratio is 2.7:1. If wetted perimeter alone were the significant factor, then the 18% penetration lobe should provide greater flame propagation. Clearly this is not the case. As has been suggested by other studies performed using non-reacting flows, the increased mixing is likely associated with the large-scale fluid motion.

If benefits are to be derived from utilizing this concept for increasing the volumetric heat release in devices, then it must be shown that the momentum loss associated with the process is small. It is always possible to achieve increased mixing at the expense of momentum loss. The feature of importance relative to this technology is that, as noted in the Introduction, it has been the case in non-reacting flow that the momentum loss is very small. The fact that there is no flow separation on the splitter surface suggests that losses should be small. In the case of a swirler, for example, separated flow at the blade root and hub produces significant loss. The

losses associated with the lobed surface can only be due to skin friction and the induced loss associated with converting axial momentum to the angular momentum of the vortices. For the configuration employing the ramped lower surface, there is a loss attributable to the base separation behind the step. That loss could be eliminated by contouring of the enclosure wall--it has been shown in ejector studies that very high angles of enclosure divergence can be employed in conjunction with lobe mixers. Although momentum loss is of high importance to application of this technology, the focus of this effort was a demonstration that high flame propagation rates can be achieved; no effort was made to quantify losses.

CONCLUSIONS

o Streamwise vorticity introduced by means of convoluted surfaces can substantially increase the rate of propagation of confined, high-speed, non-premixed flames.

o The highly asymmetric, extreme aspect ratio lobes required for mixing streams having large flow area differences (7:1) can produce intense large-scale streamwise vortex arrays, but the enclosure geometry plays a critical role in the vortex development.

o In streamwise-vorticity stirred flows, either hot or cold, the effect of velocity ratio on mixing was small. In hot flow, the effect of initial stream temperature and of equivalence ratio was small. If the vortex array is produced for one condition through appropriate lobe and enclosure design, then the enhanced mixing will be observed over a wide range of flow conditions.

RECOMMENDATIONS

o Experiments should be conducted to evaluate the momentum loss associated with the application of the concept to high-subsonic-speed, high-heat-release flows.

o Experimental data should be acquired and analytical procedures developed to permit prediction of the effect of convoluted surface design parameters and enclosure geometry on vortex array development. Because the vortex development process is dominated by inviscid effects, and not by turbulent transport, analytical treatment should be well within current capabilities. Cold flow experiments would be suitable.

o The processes of importance to the application of this concept to combustion devices should be investigated. In particular, the means of controlling the interaction between the intensely-mixing vortex array and the flame stabilization sites, where rapid mixing can degrade performance, should be addressed.

REFERENCES

Bevilaqua, P. M.: An Evaluation of Hypermixing for VSTOL Aircraft Augmentors, AIAA Paper 73-654, 1973.

Bray, K. N. C. and P. A. Libby: Interaction Effects in Turbulent Premixed Flames, Physics of Fluids. Vol. 19 (1976), pp. 1687-1701.

Gutmark, E., K. C. Schadow, T. P. Parr, D. M. Parr and K. J. Wilson: Combustion Enhancement by Axial Vortices. AIAA Paper 87-1831, June 1987.

Paterson, R. W.: Turbofan Mixer Nozzle Flow Field - A Benchmark Experimental Study. Journal of Engineering for Gas Turbines and Power. Vol. 106 (1984).

Presz, W., R. Gousy and B. Morin: Forced Mixer Lobes in Ejector Designs. AIAA Paper 86-1614 (1986).

Rogers, T. and J. G. Bendot: AFT Inlet/Hypermixing Ejector Technology Program. Air Force Aeropropulsion Laboratory Report AFAPL-TR-76-79), August 1976.

Skebe, S. A., R. W. Paterson, and T. J. Barber: Experimental Investigation of Three-Dimensional Forced Mixer Lobe Flow Fields. AIAA Paper 88-3785, July 1988.

Spalding, D. B.: The Spread of Turbulent Flames Confined in Ducts. Eleventh Symposium (International) on Combustion, (1967), pp. 807-815.

Werle, M. J., R. W. Paterson and W. M. Presz: Flow Structure in a Periodic Vortex Array. AIAA Paper 87-0610 (1987).

Williams, G. C., H. C. Hottel, and A. C. Scurlock. Flame Stabilization and Propagation in High Velocity Gas Streams. Third Symposium on Combustion (1949), p. 49.

Wright, F. H. and E. E. Zukoski: Flame Spreading from Bluff-Body Flameholders. Eighth Symposium (International) on Combustion (1962), p. 933.

Flow deflection (Inviscid)

Flow separation (Viscous)

Vortex rollup
(Inviscid)

Vortex breakdown
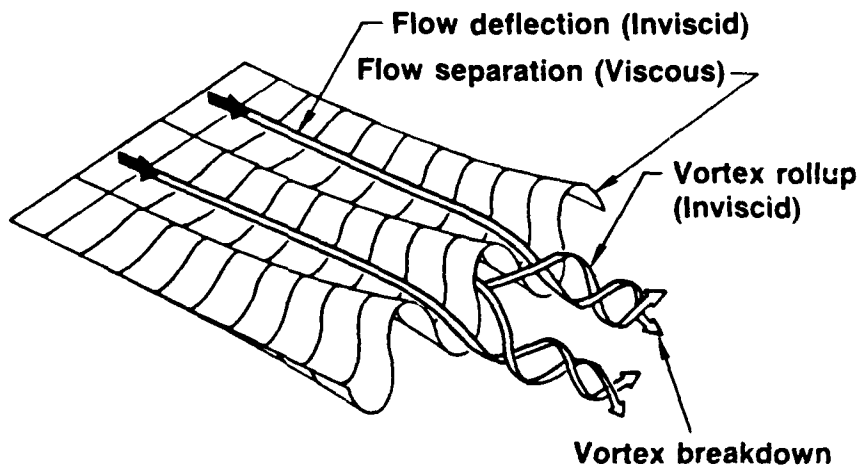
Fig. 1   Streamwise vorticity generation by a convoluted flow splitter.

Profile

α

Pitch

Aspect
ratio
(H/W)

H

W

Confinement

Penetration
(A/B)

B

H

Shape
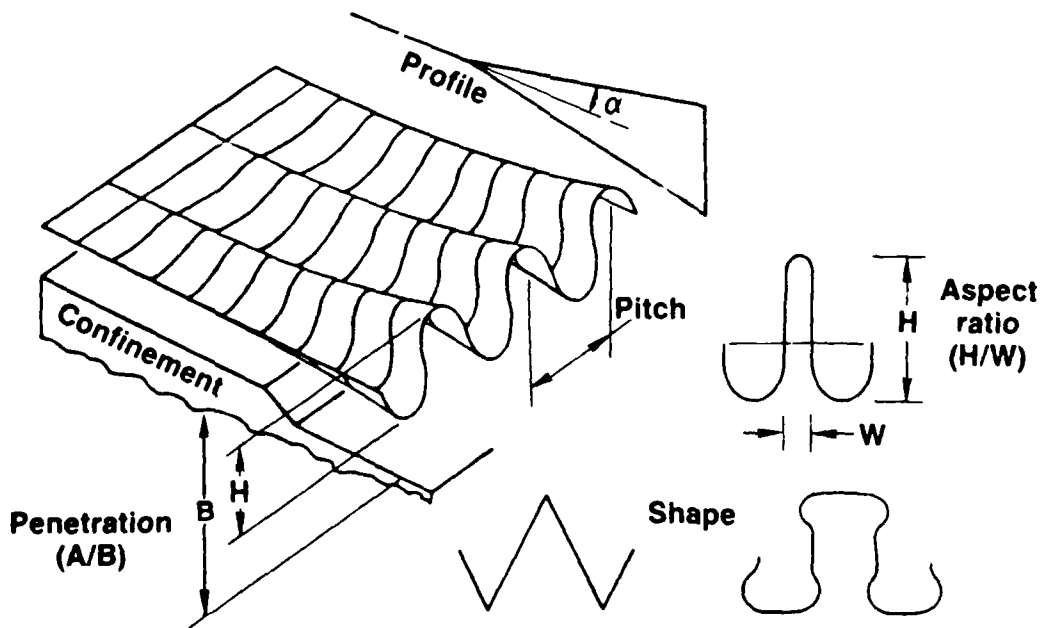
Fig. 2   Geometric factors affecting vorticity development.

16.5 cm width

14 cm height

Secondary flow

Primary flow
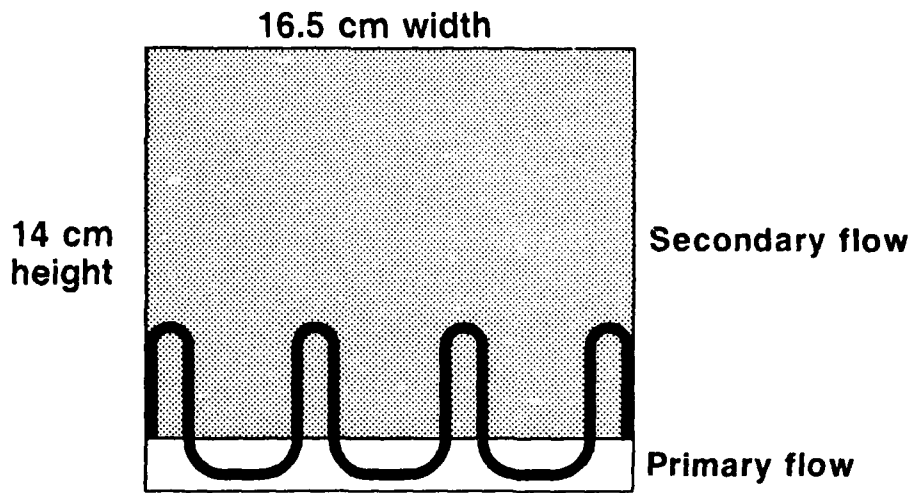
Area ratio - 7:1   Primary aspect ratio - 5:1

Penetration - 35%   Secondary aspect ratio - 1.5:1

Fig. 3   High-penetration lobed mixer.
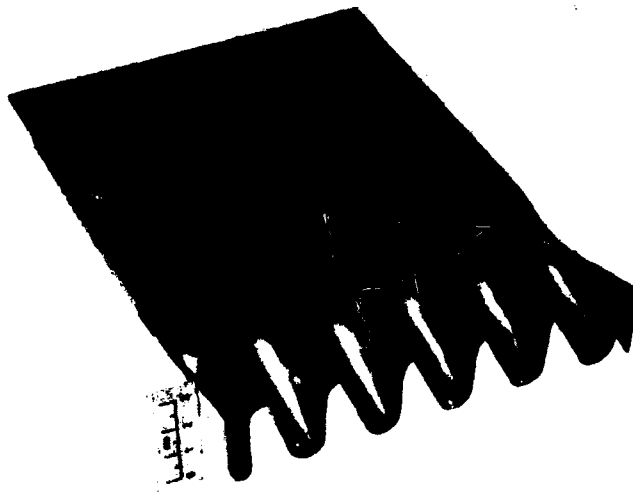
Penetration-18%   Primary aspect ratio 2:1
Secondary aspect ratio 2:1

Fig. 4   Low penetration lobed mixer.

88—8—27—2
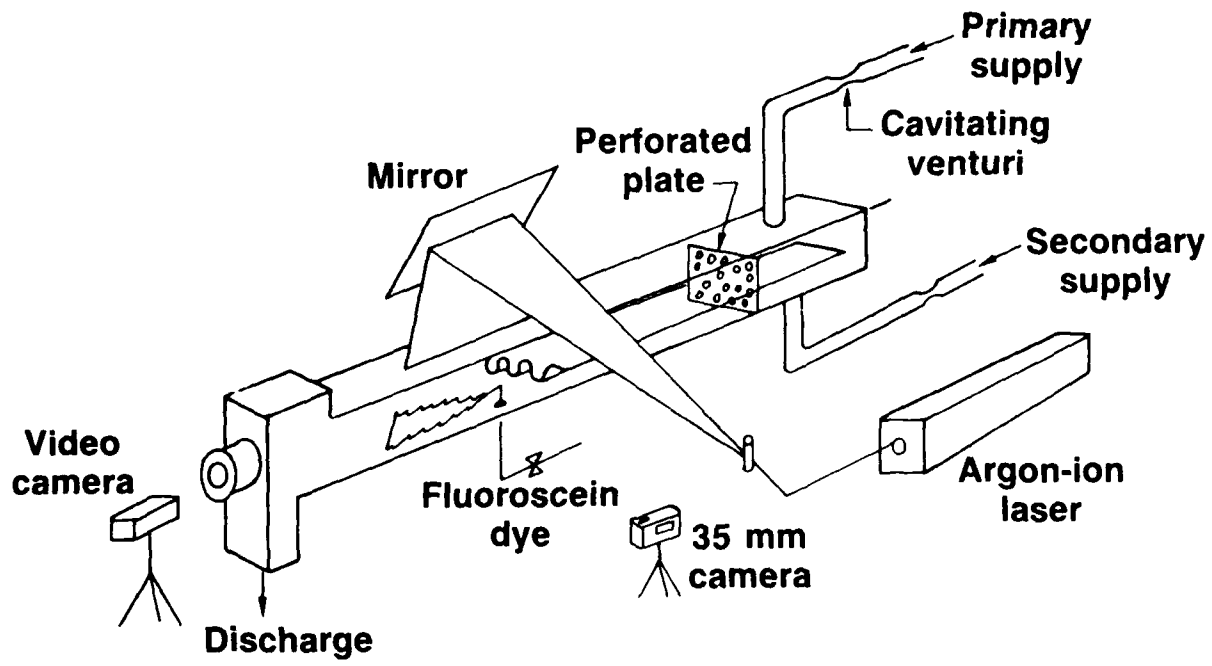
a) SCHEMATIC DIAGRAM OF TEST APPARATUS
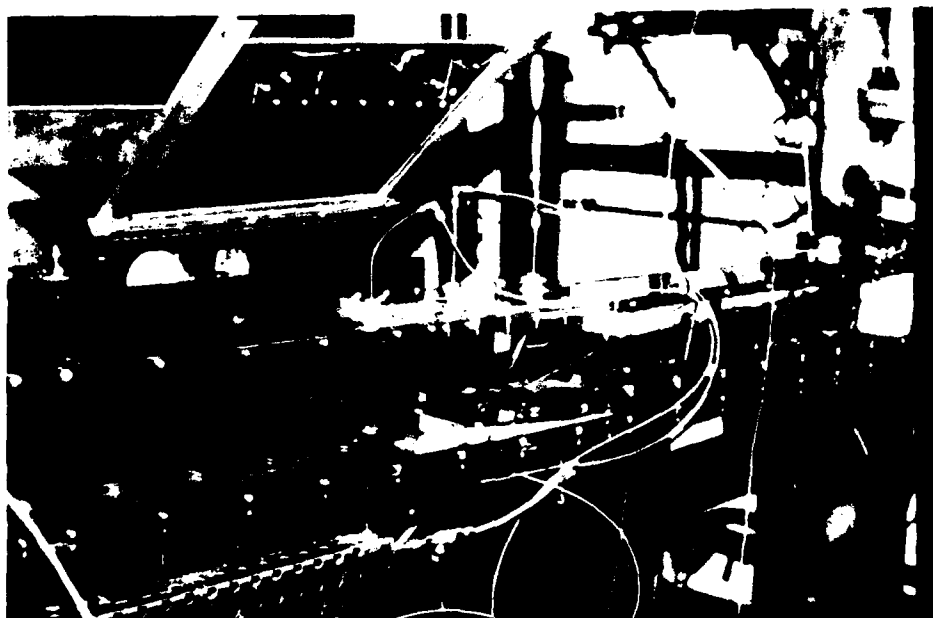
b) VIEW OF TEST SECTION

Fig. 5   Water flow visualization test facility.

Primary flow →
$dA/dX = 0$

Secondary flow →
$dA/dX = 0$

a) Without ramp

$dA/dX < 0$

$dA/dX = 0$

2 cm

7.1 deg
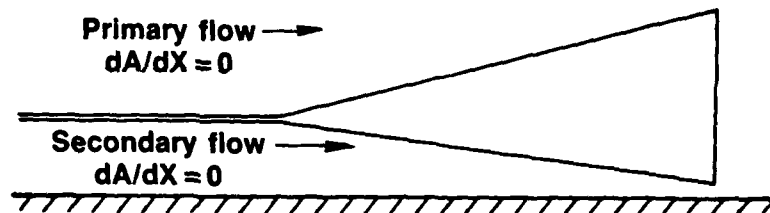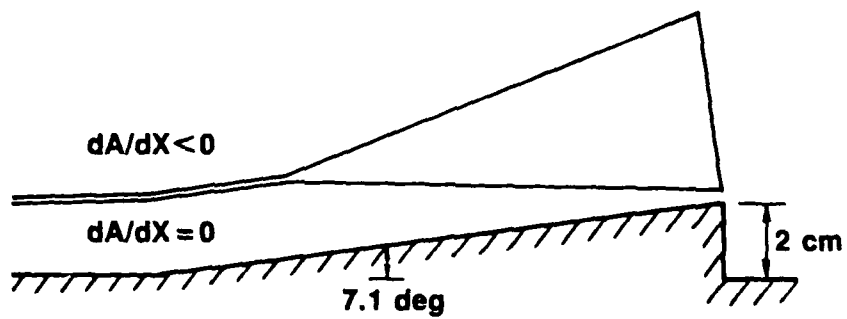
b) With ramp

Fig. 6   Lobe installation details.
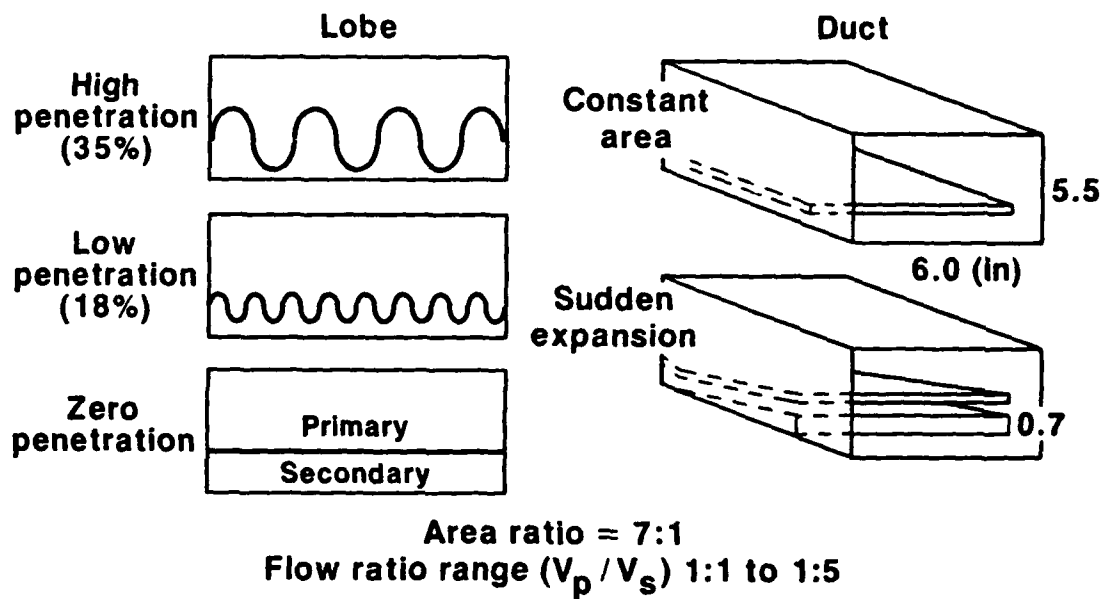
Fig. 7   Flow visualization test configurations.

Primary
flow
(seeded)

Secondary
flow
(unseeded)

Base of ramp
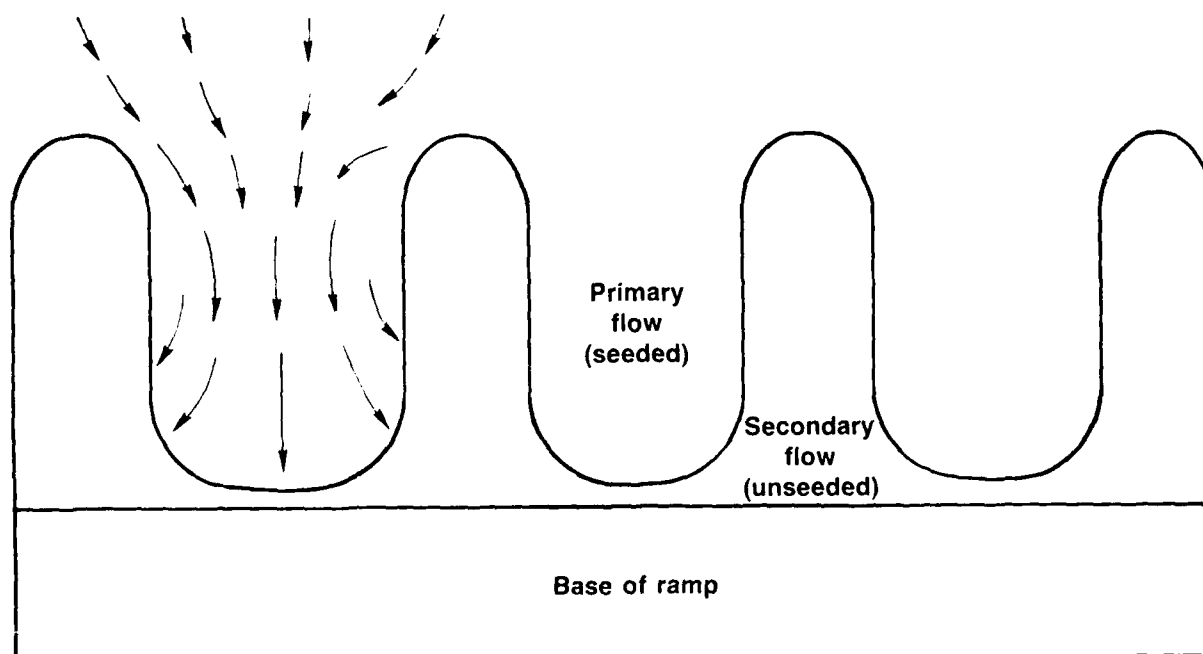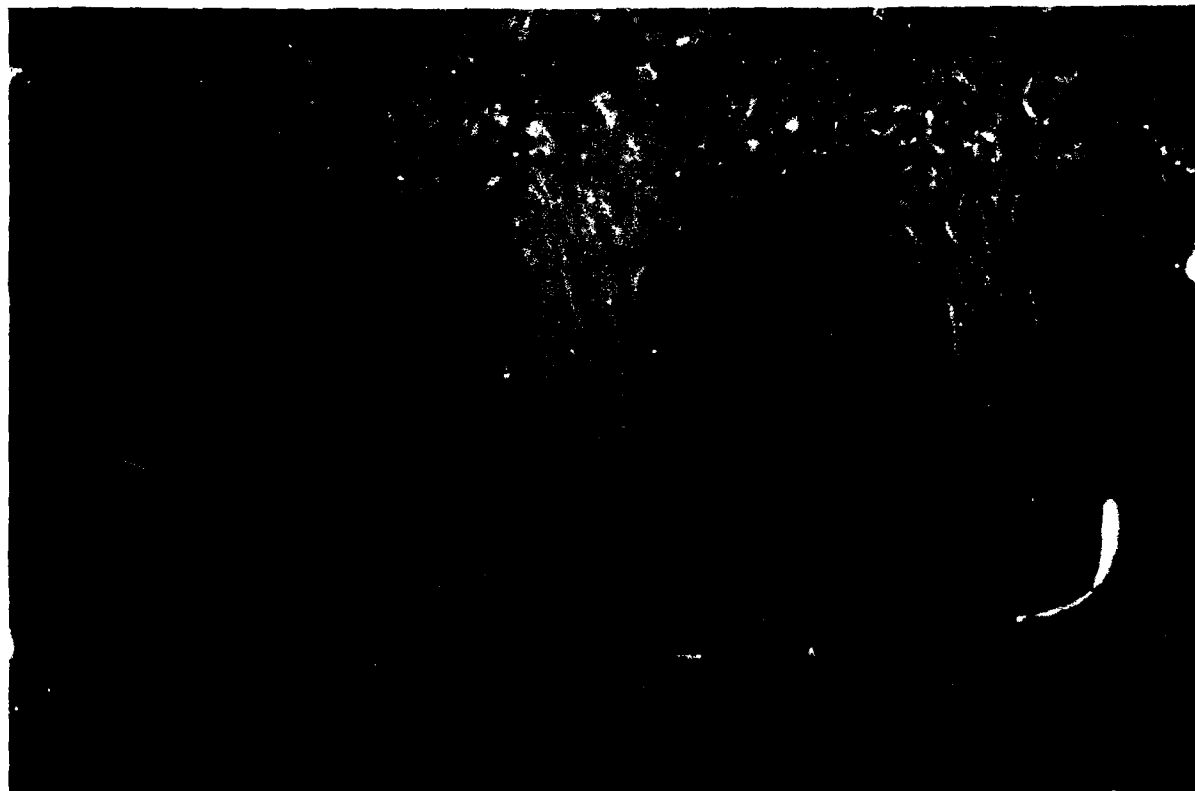
Fig. 8   Flow visualization showing large scale vortex array downstream of lobed mixer.

Primary
flow
(unseeded)

Secondary
flow
seeded

Base of ramp
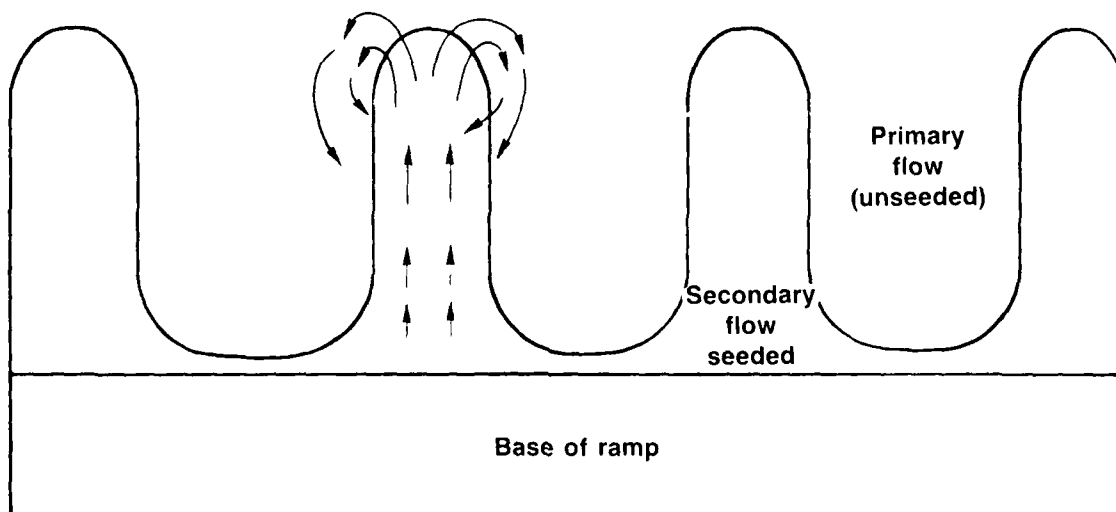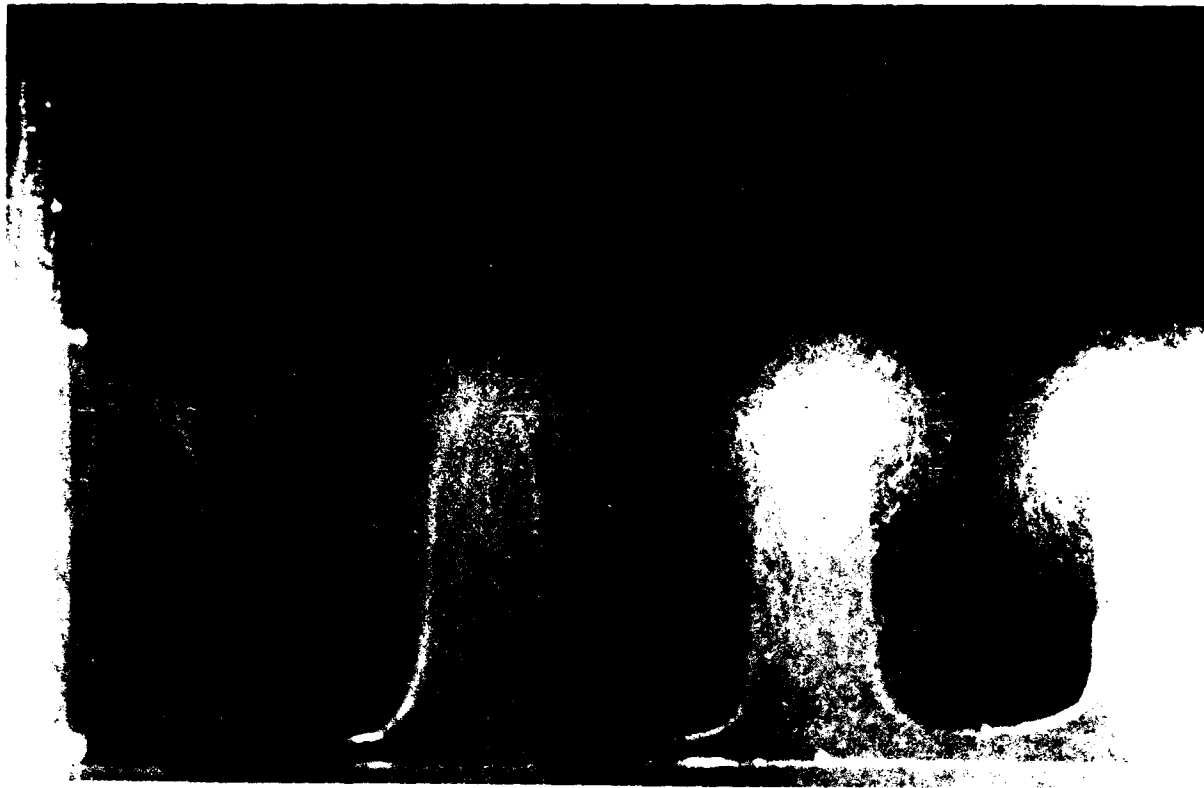
Fig. 9   Exit plane visualization showing vortex rollup process.
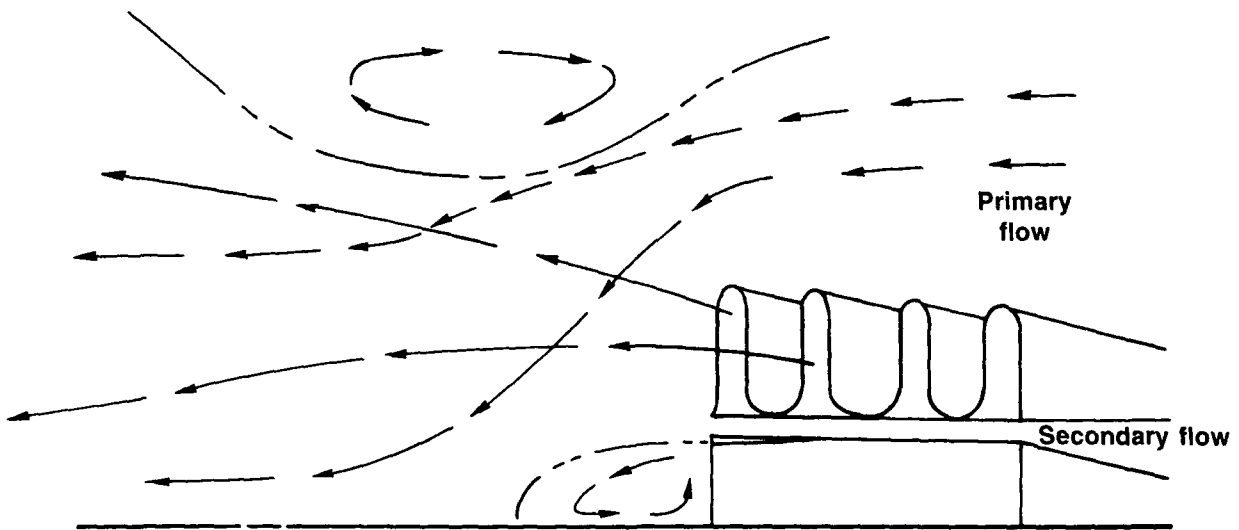
Fig. 10 Dye trace flow visualization showing rapid turning of primary flow.
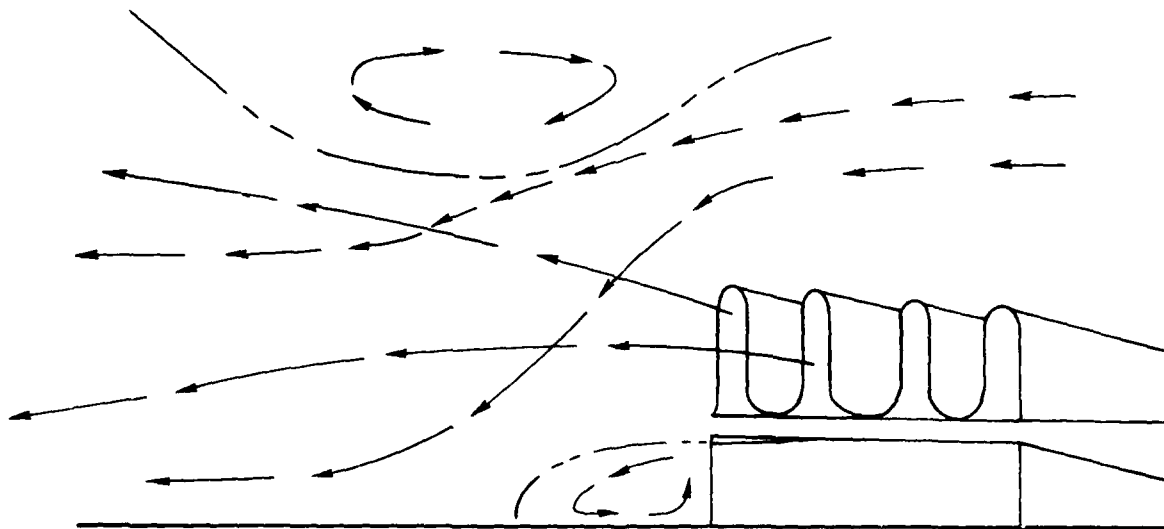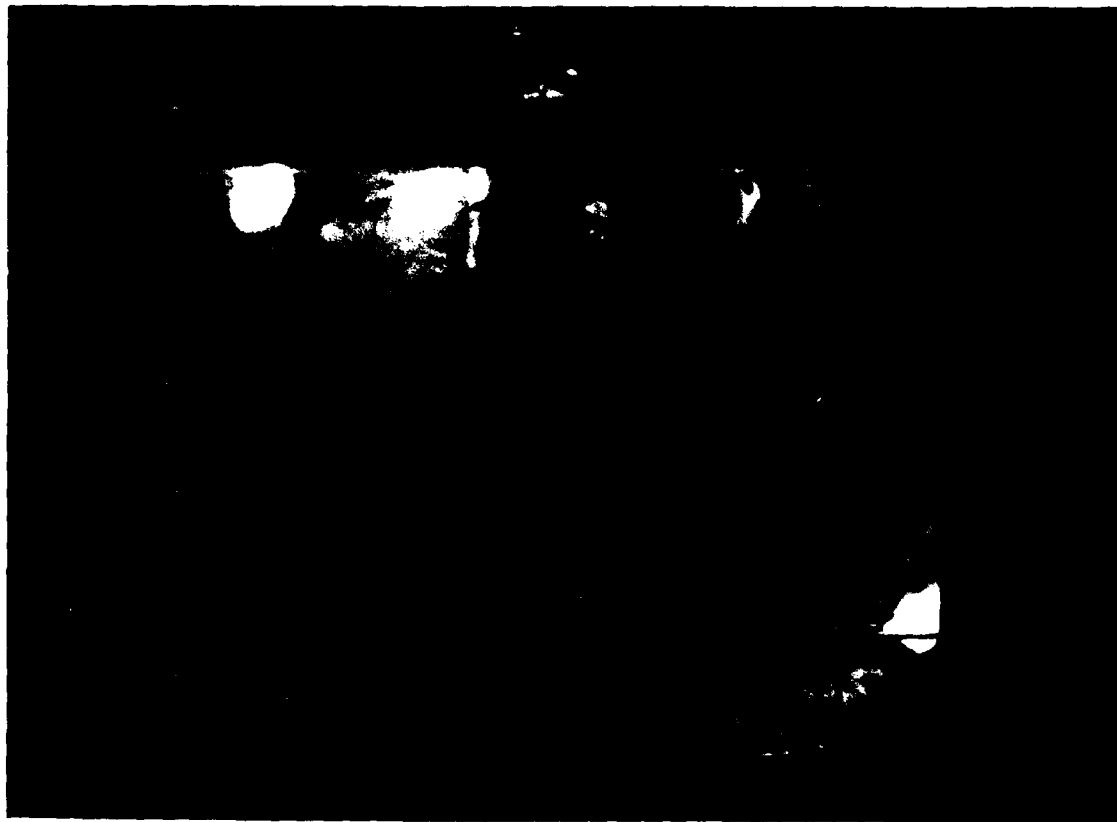
Fig. 11 Dye trace flow visualization showing separated flow regions.
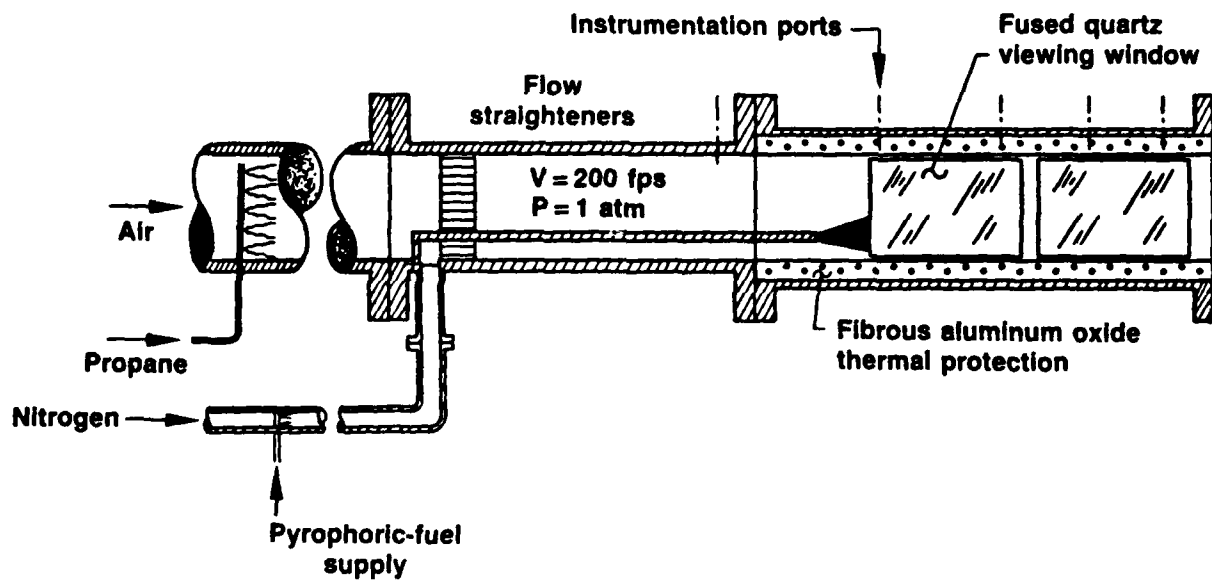
Fig. 12   Schematic diagram of test apparatus.
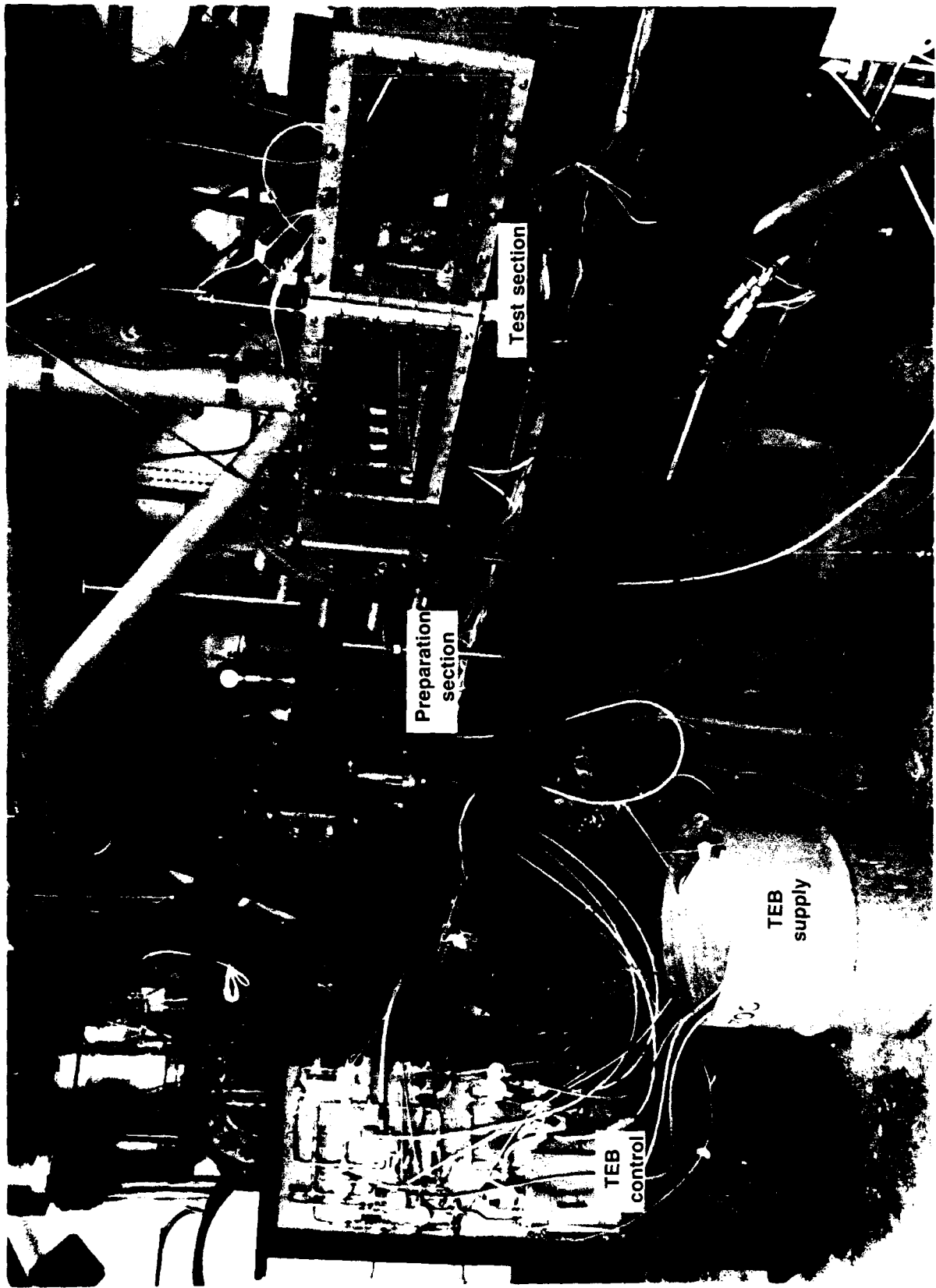
Fig. 13 Overall view of combustion test apparatus.

Test section

Preparation section

TEB supply

TEB control

88—8—27—10
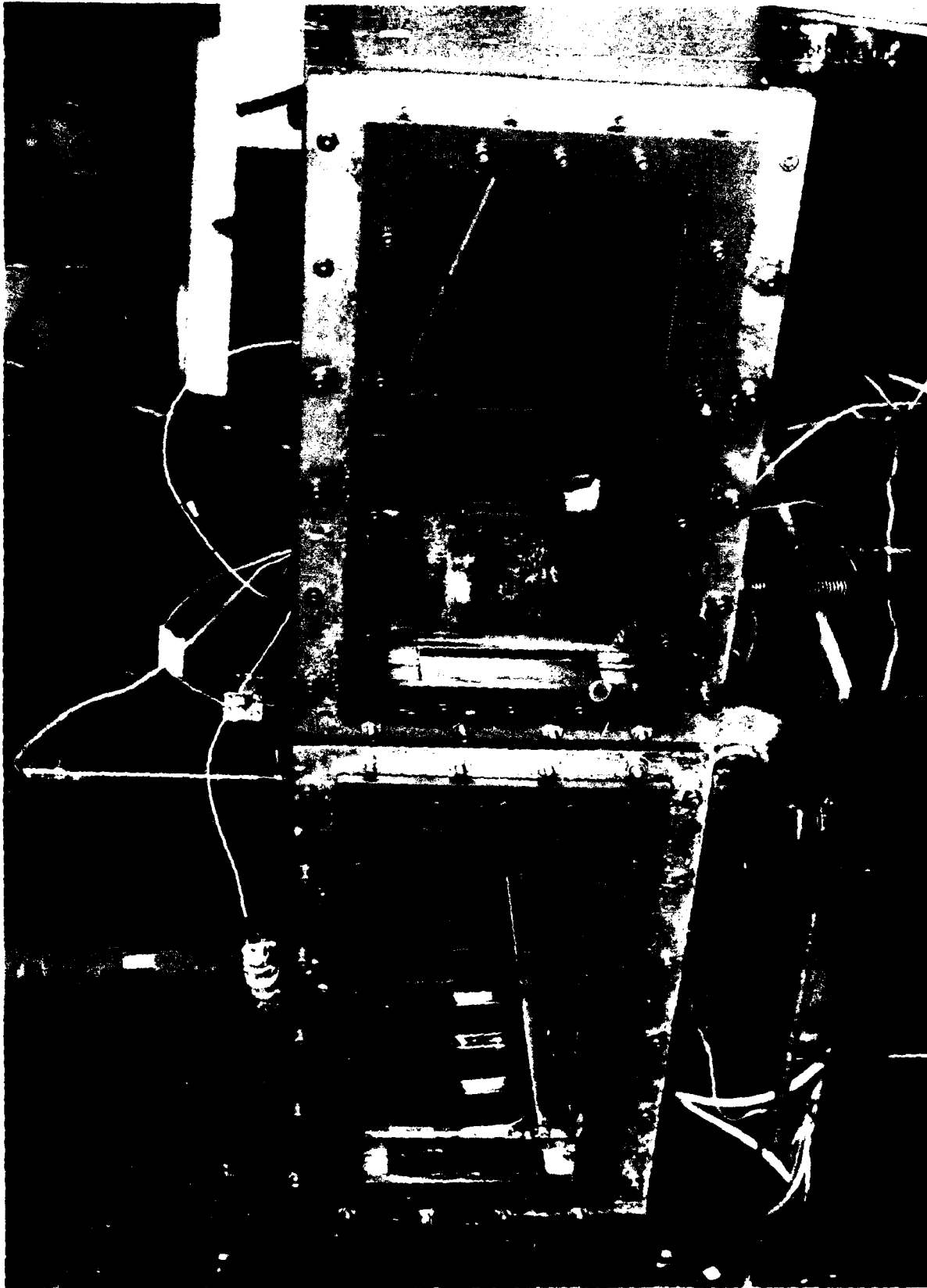
Fig. 14 Close-up view of test section.

88—92—A5

88—8—27—11

FLAT PLATE TEST 49

PRIMARY VELOCITY = 45.72 m/sec SECONDARY VELOCITY = 9.91 m/sec TEB FLOW RATE = 0.59 kg/min

COVERAGE = 46%

FLAT PLATE WITH RAMP TEST 120

PRIMARY VELOCITY = 30.48 m/sec SECONDARY VELOCITY = 45.72 m/sec TEB FLOW RATE = 1.04 kg/min

COVERAGE = 52%

18% PENETRATION LOBE TEST 52

PRIMARY VELOCITY = 45.72 m/sec SECONDARY VELOCITY = 9.91 m/sec TEB FLOW RATE = 0.59 kg/min

COVERAGE = 59%

35% PENETRATION LOBE TEST 56

PRIMARY VELOCITY = 45.72 m/sec SECONDARY VELOCITY = 9.91 m/sec TEB FLOW RATE = 0.59 kg/min

COVERAGE = 62%
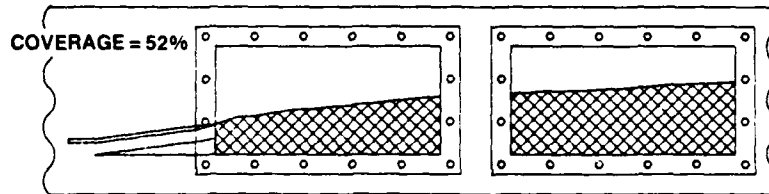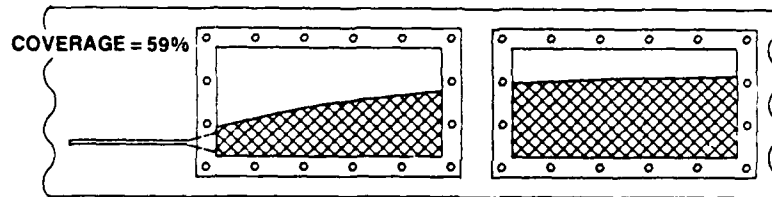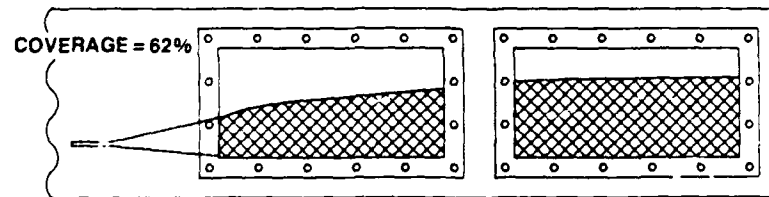
35% PENETRATION LOBE WITH RAMP TEST 137

PRIMARY VELOCITY = 45.72 m/sec SECONDARY VELOCITY = 5.1 m/sec TEB FLOW RATE = 0.92 kg/min

COVERAGE = 84%
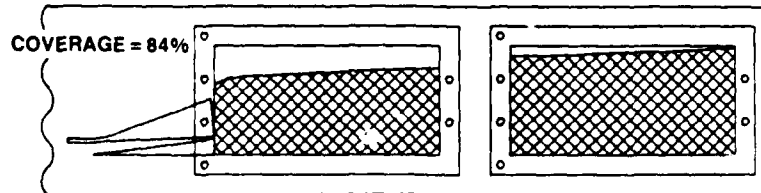
Fig. 15 Flame envelope derived from digitized photographs.

88—8—27—23
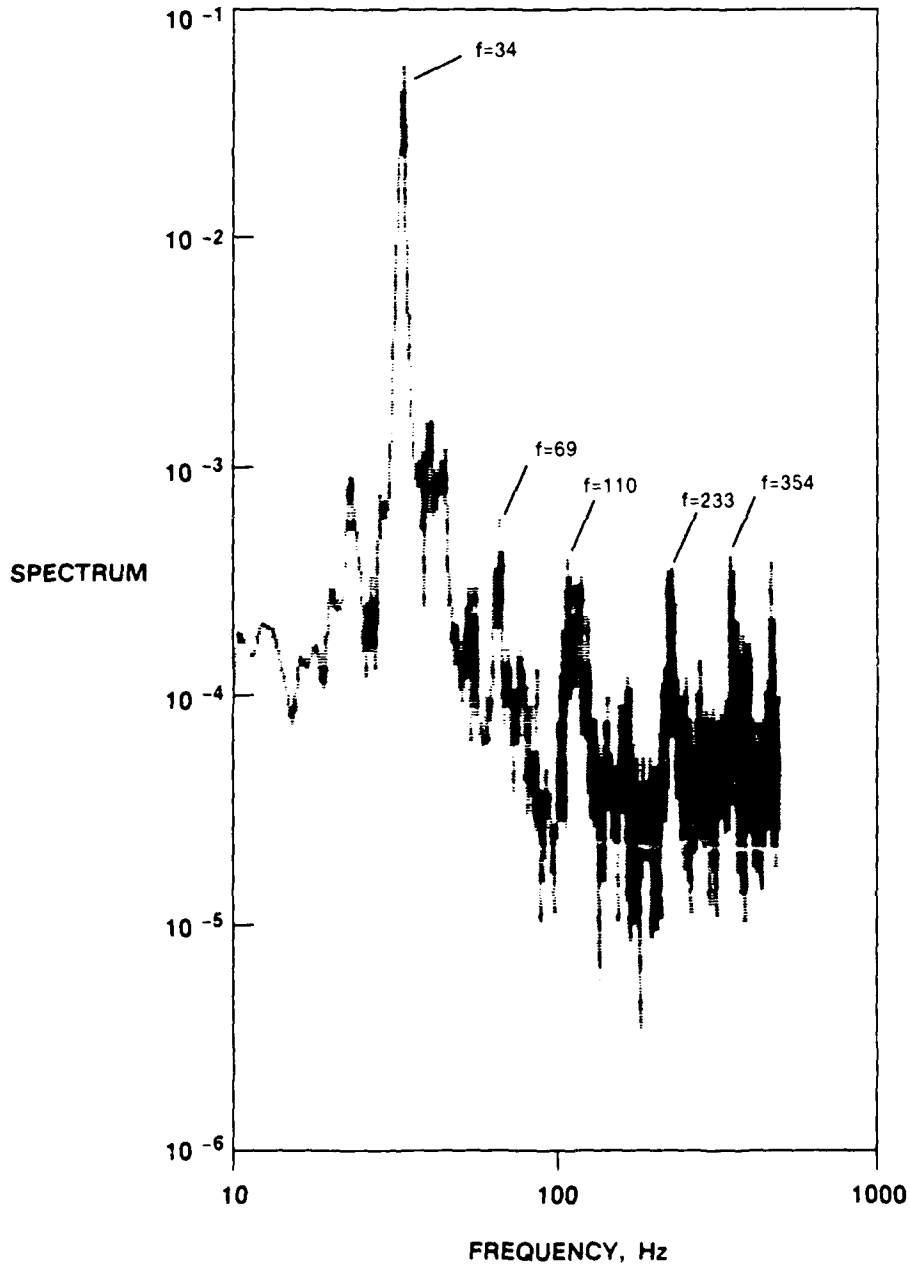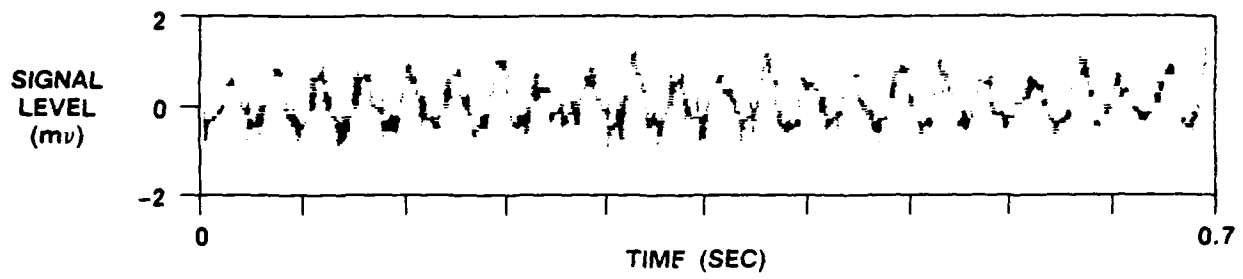
Fig. 16 Pressure oscillation – Test 88.
(V_{psi} = 26.8mps. V_{psi}/V_{sec} =1.2, ϕ = 0.31)

88-8-27-18
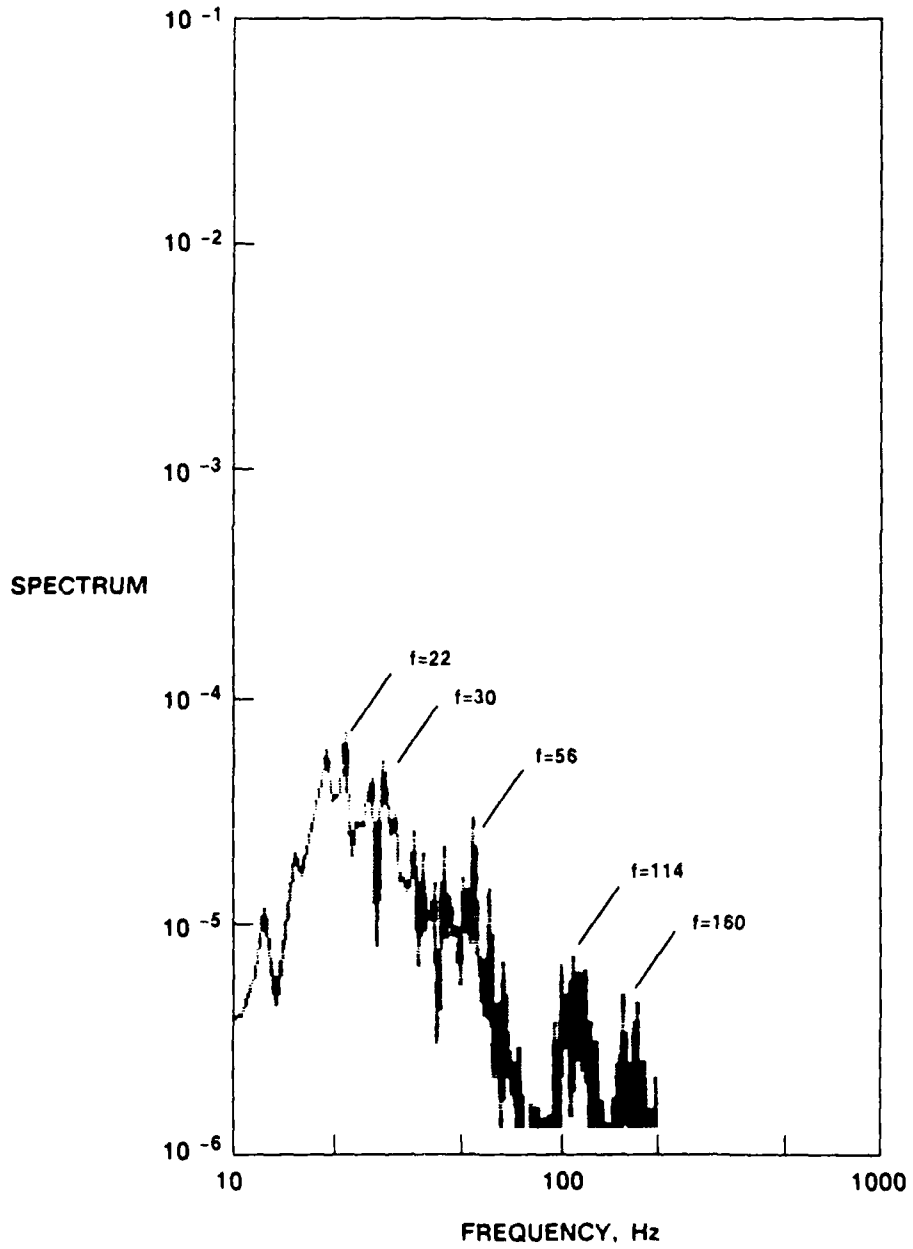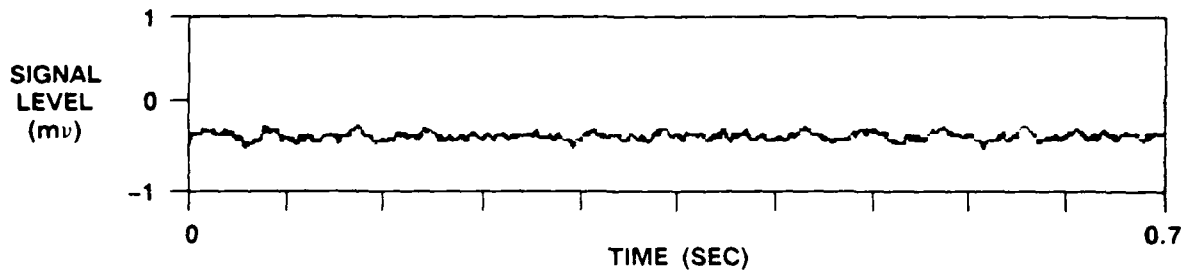
Fig. 17 Pressure characteristic – Test 125.

(V= 45.7 m/sec, V_{psi}/V_{sec} = 1.5, 0 = 0.31)
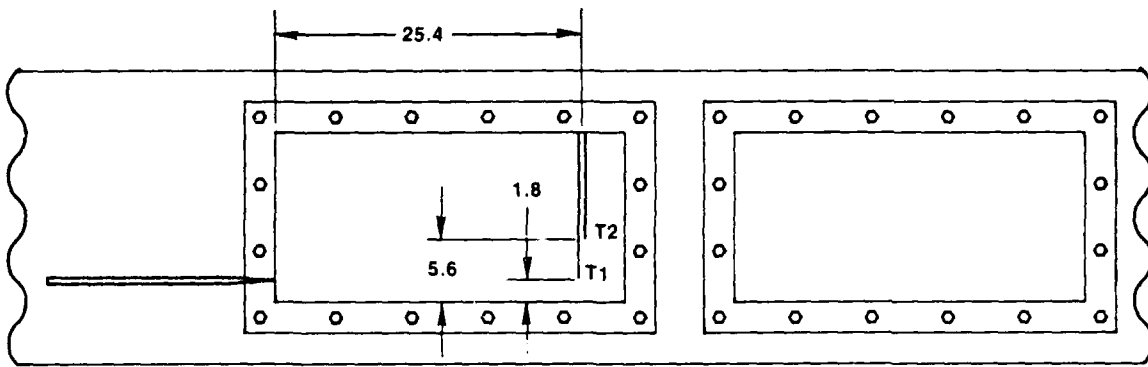
CONFIGURATION A
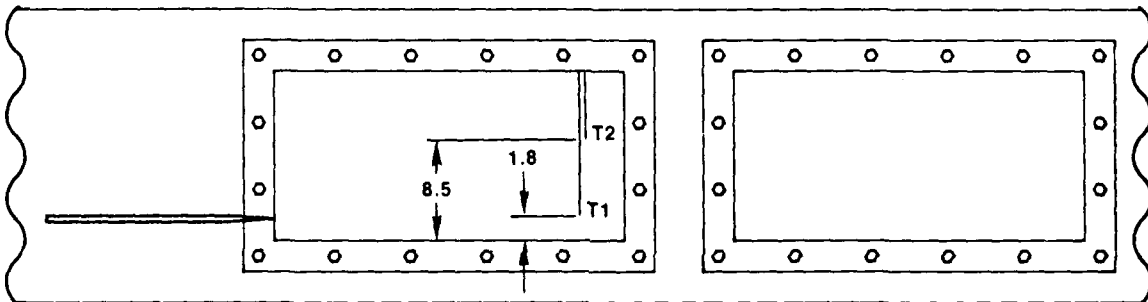
CONFIGURATION B
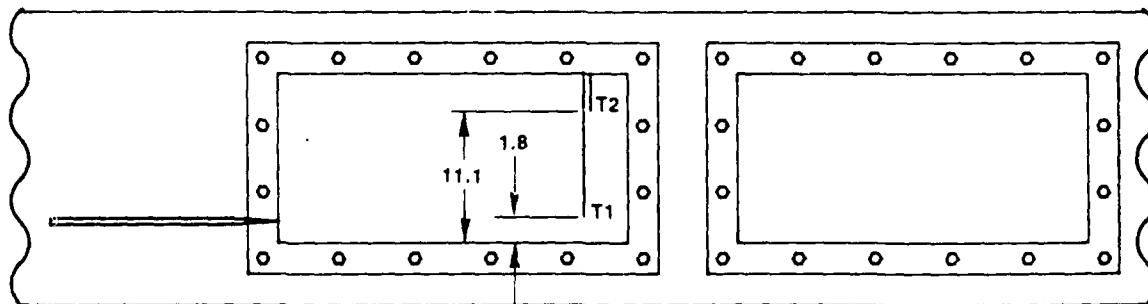
CONFIGURATION C

Fig. 18   Thermocouple locations.

88—8—27—12

FLAT PLATE WITH RAMP   TEST 120

V PRI = 30.5 M/SEC   VPRI/VSEC = .7   PHI = .43
T1○—○—○   T2▷—▷—▷

FLAT PLATE WITH RAMP   TEST 121

V PRI = 30.5 M/SEC   VPRI/VSEC = 1   PHI = .44
T1○—○—○   T2▷—▷—▷

FLAT PLATE WITH RAMP   TEST 123

V PRI = 45.7 M/SEC   VPRI/VSEC = 3   PHI = .3
T1○—○—○   T2▷—▷—▷

FLAT PLATE WITH RAMP   TEST 128

V PRI = 61 M/SEC   VPRI/VSEC = 2   PHI = .23
T1○—○—○   T2▷—▷—▷
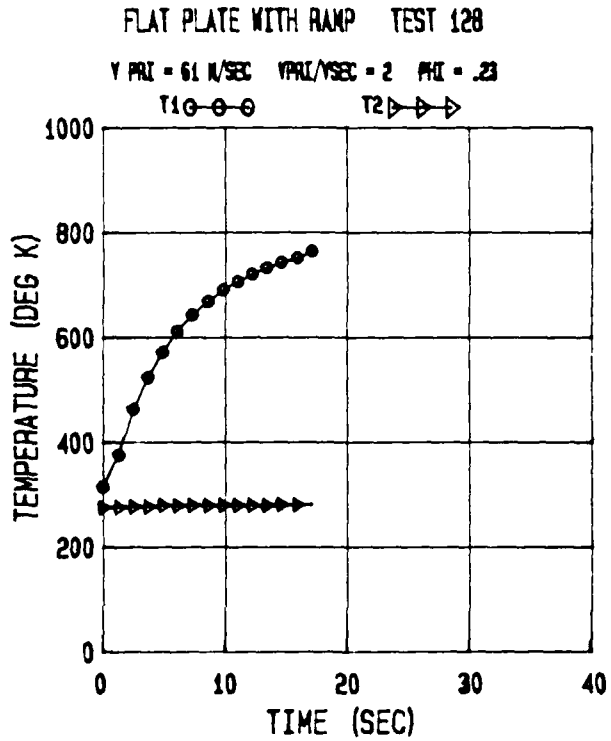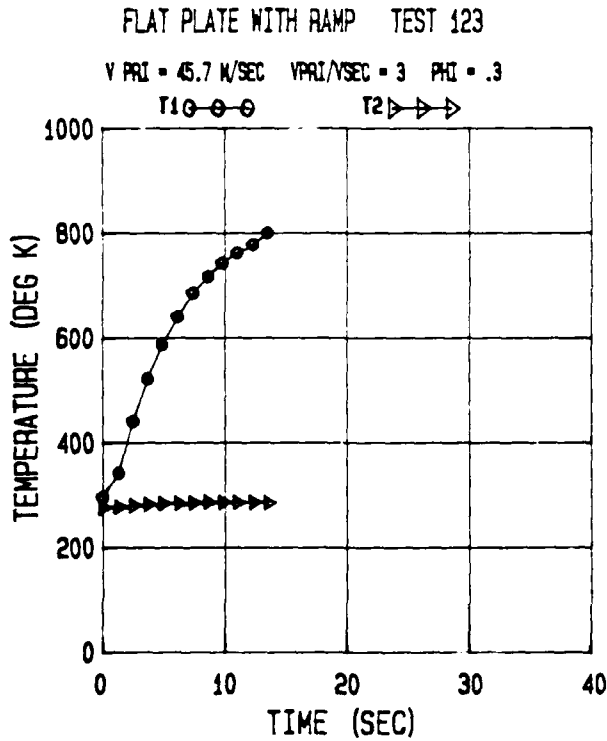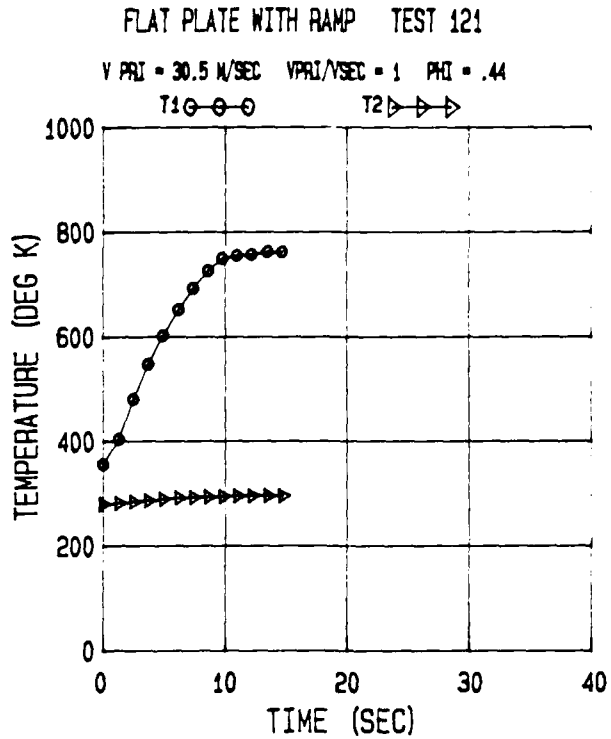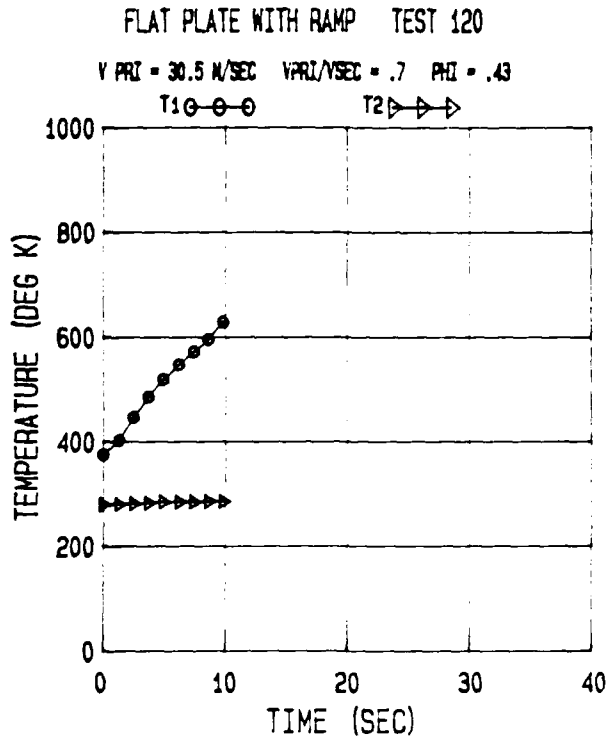
Fig. 19   Thermocouple response to combustion — flat plate.

88—8—27—13

35% PENETRATION LOBE WITH RAMP   TEST 137

V PRI = 45.7 M/SEC   VPRI/VSEC = 3   PHI = .26

T1⊖—⊖—⊖   T2▷—▷—▷

35% PENETRATION LOBE WITH RAMP   TEST 134

V PRI = 45.7 M/SEC   VPRI/VSEC = 1.5   PHI = .27

T1⊖—⊖—⊖   T2▷—▷—▷

35% PENETRATION LOBE WITH RAMP   TEST 142

V PRI = 61 M/SEC   VPRI/VSEC = 4   PHI = .13

T1⊖—⊖—⊖   T2▷—▷—▷

35% PENETRATION LOBE WITH RAMP   TEST 144

V PRI = 61 M/SEC   VPRI/VSEC = 4   PHI = .12

T1⊖—⊖—⊖   T2▷—▷—▷
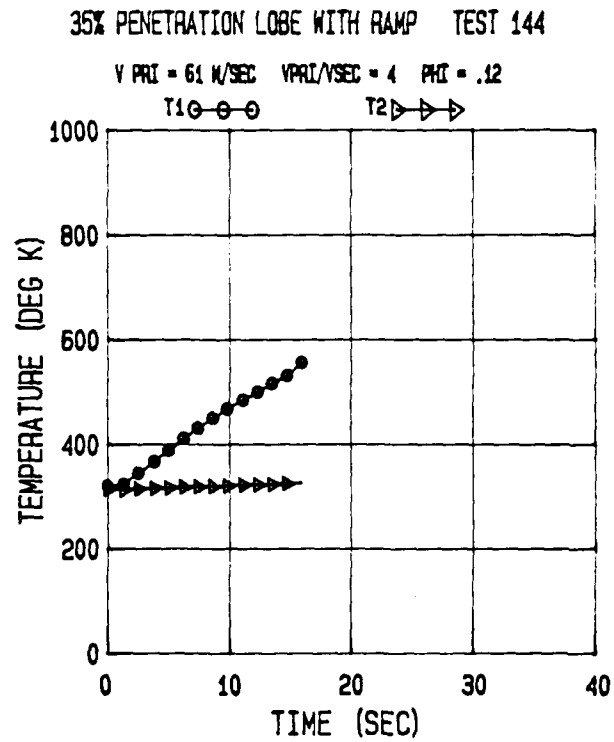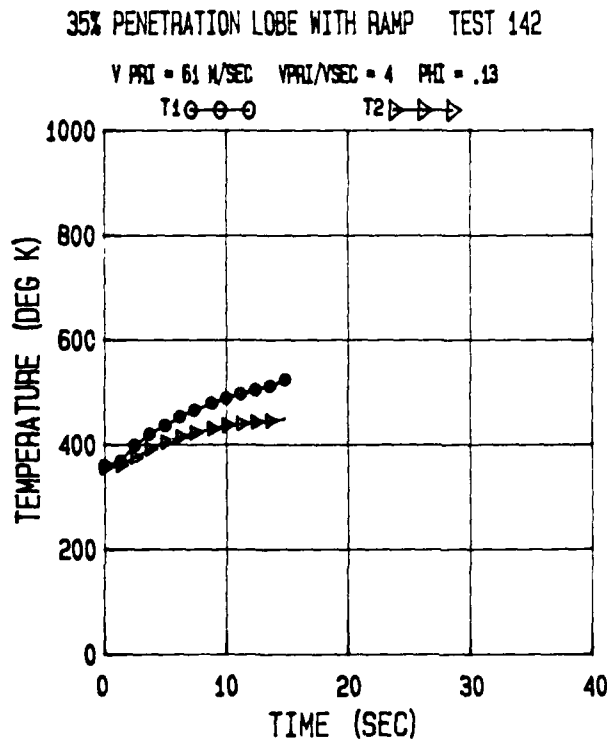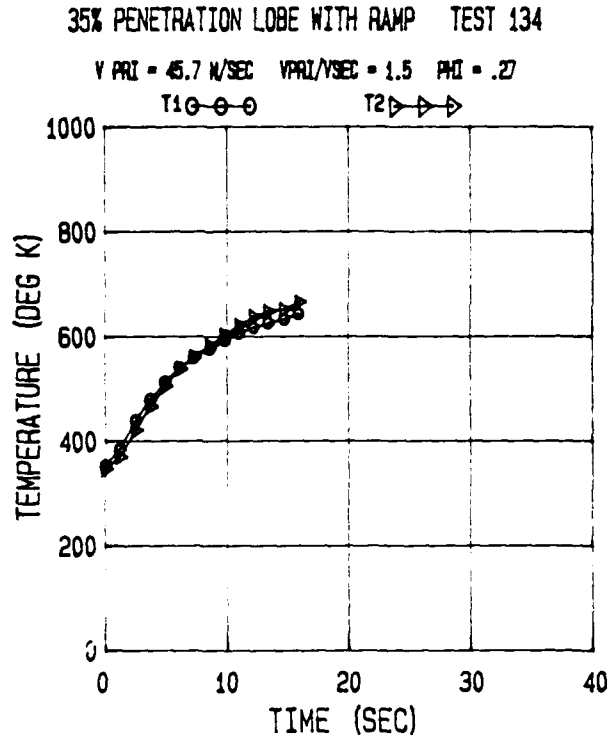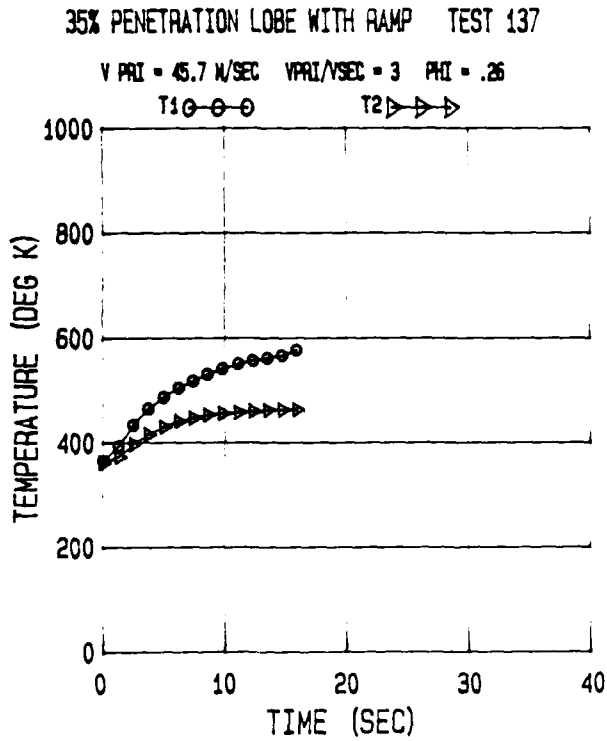
Fig. 20   Thermocouple response to combustion — 35% penetration lobe with ramp.

88—8—27—14
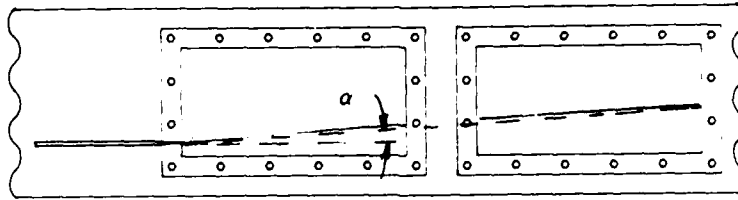
FLAT PLATE

FLAT PLATE WITH RAMP
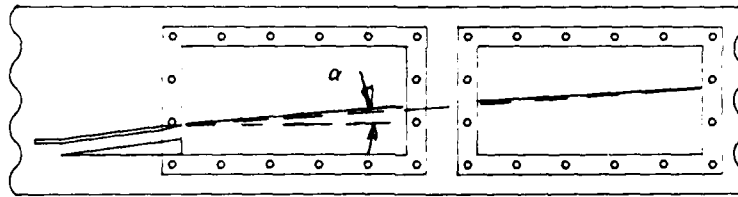
18% PENETRATION LOBE
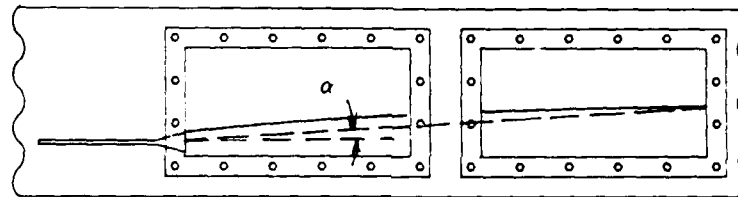
35% PENETRATION LOBE
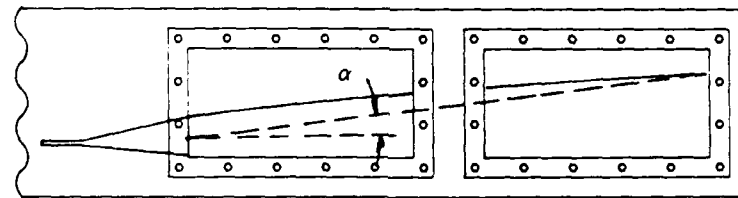
35% PENETRATION LOBE WITH RAMP
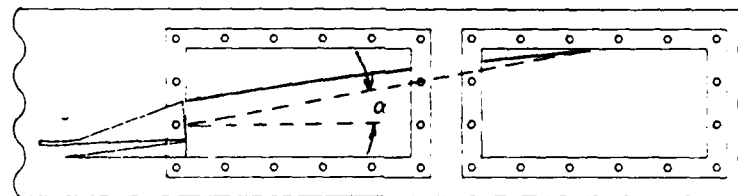
Fig. 21   Definition of flame spreading angle, α.
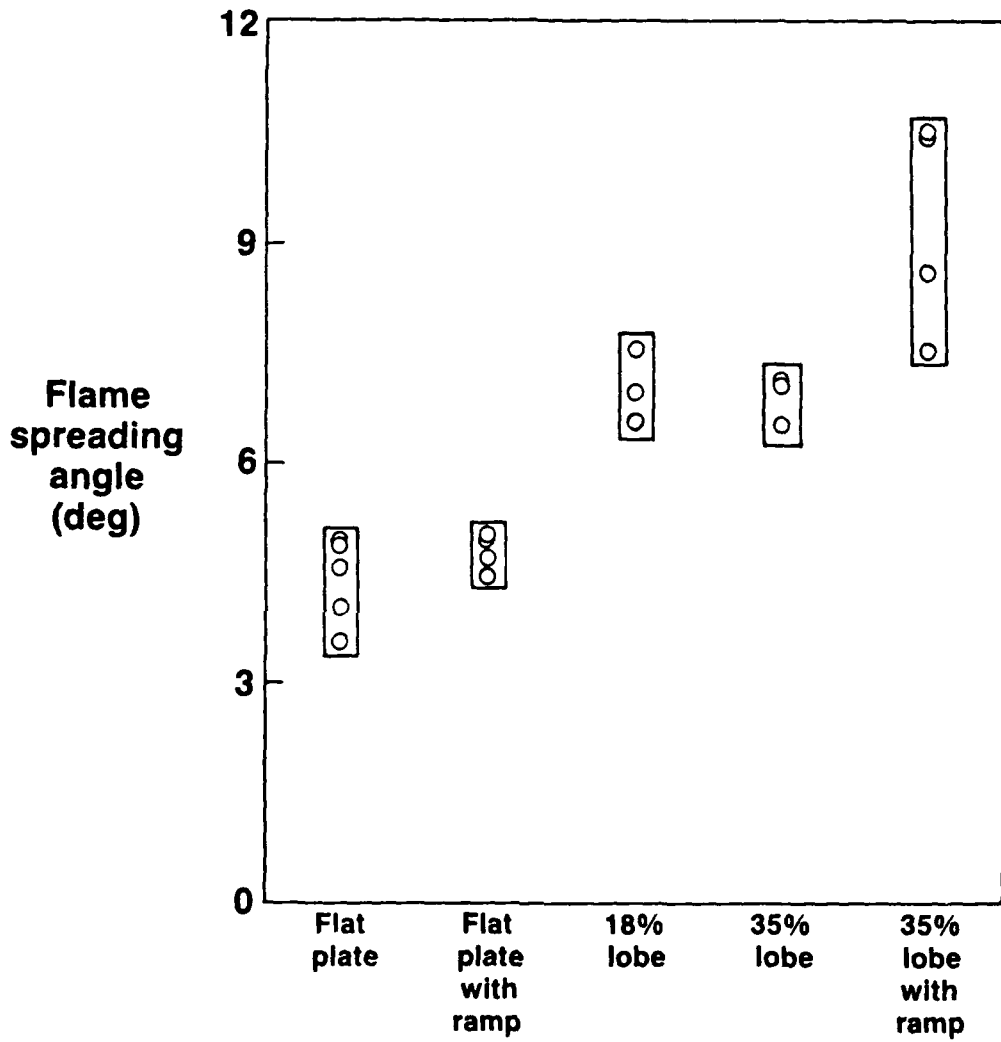
Fig. 22   Effect of convoluted splitter design on flame spreading rate.

Plate 1. Test apparatus view as recorded by the 35mm camera.

88—8—27—29

$V_{PRIMARY} = 45.7$ m/s
$V_{pri}/V_{sec} = 4.6$
EQUIVALENCE RATIO $= 0.16$

88—8—27—30
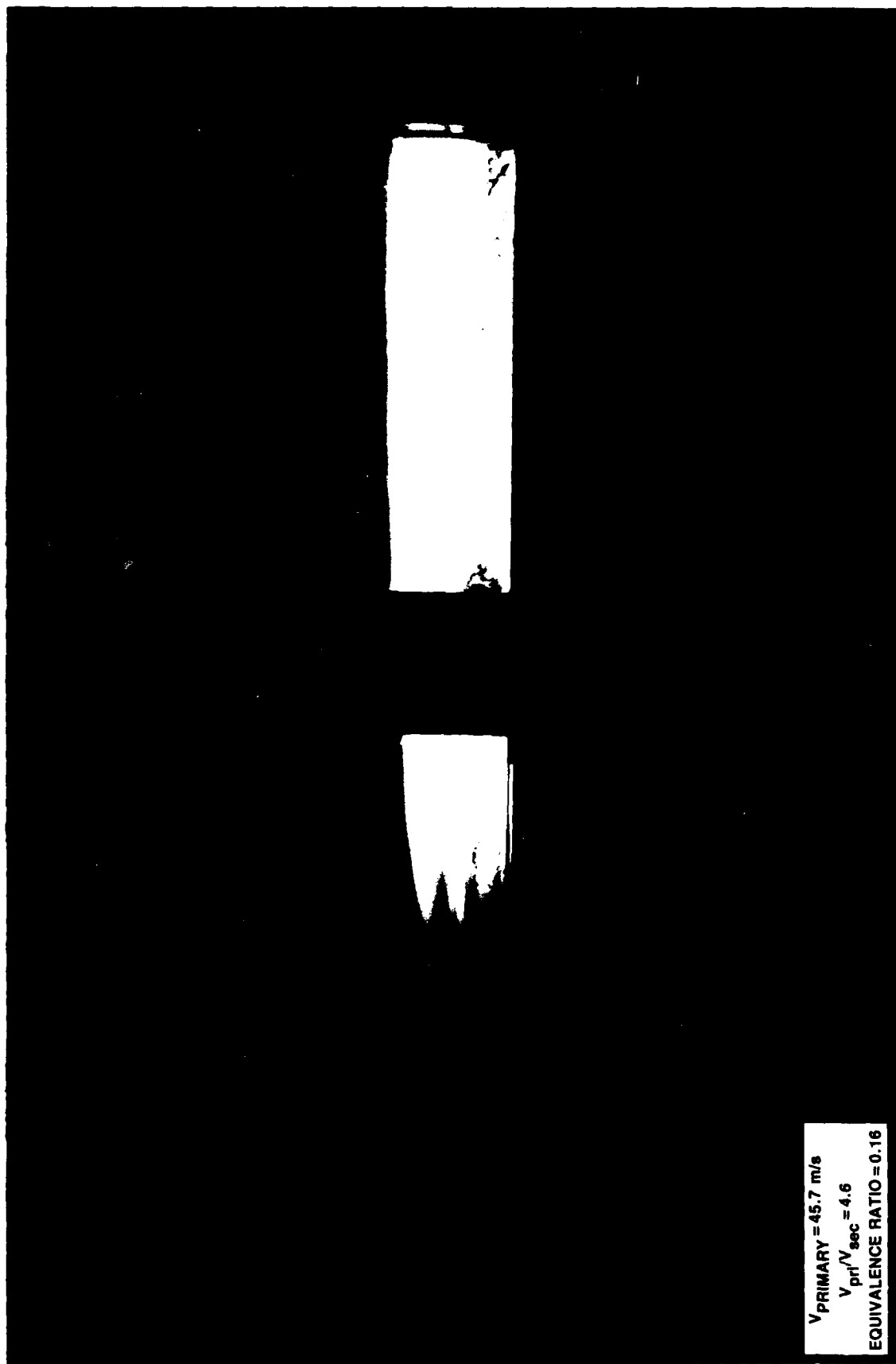
Plate 2.   Flame photograph — flat plate (test 49).

V_PRIMARY = 45.7 m/s

V_{prf}/V_{sec} = 4.6
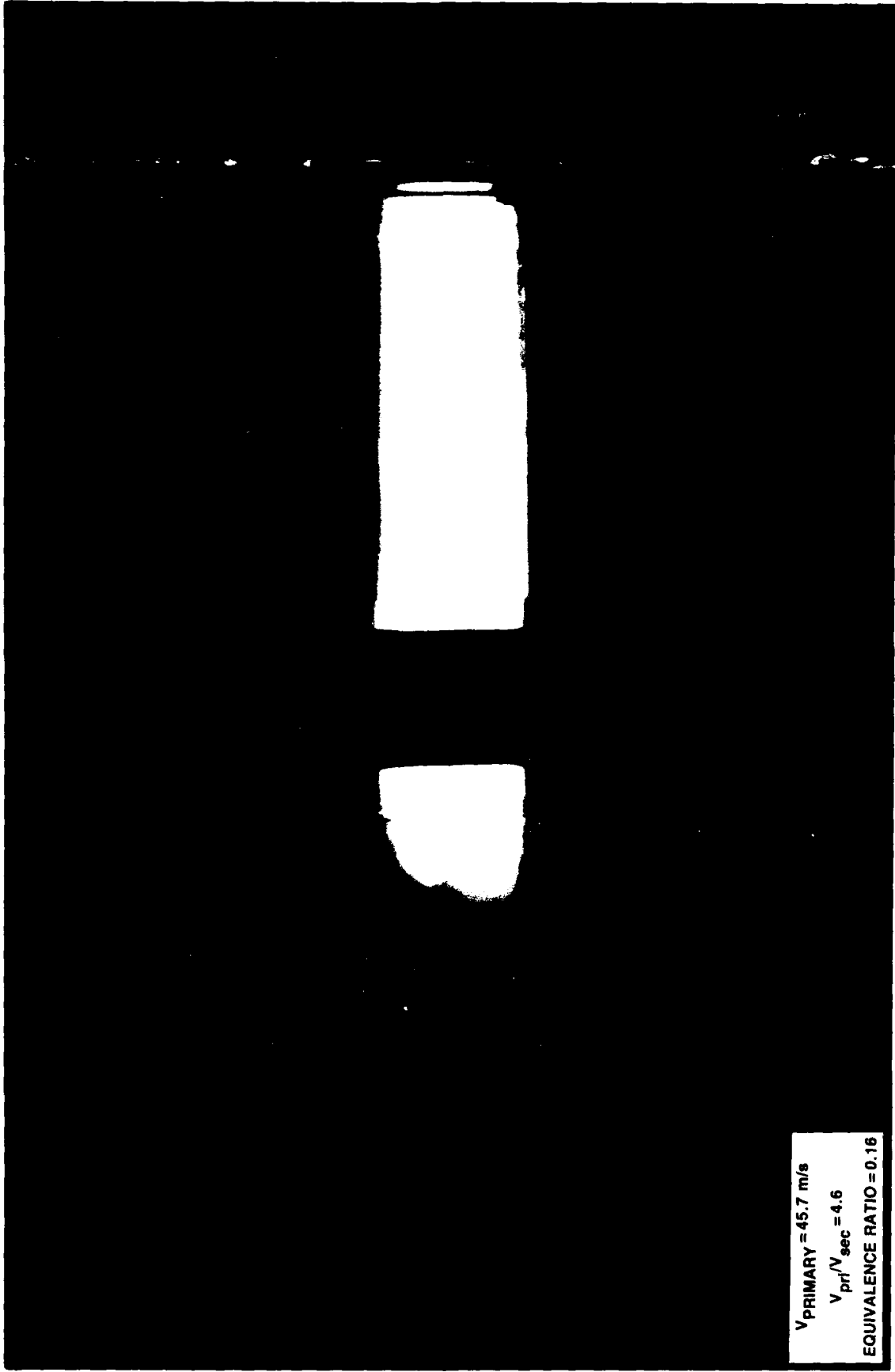
EQUIVALENCE RATIO = 0.16

Plate 3.   Flame distortion due to combustion oscillation — 18% penetration lobe (test 51).

88—8—27—31

$V_{PRIMARY} = 30.3$ m/s
$V_{pri}/V_{sec} = 0.7$
EQUIVALENCE RATIO = 0.43

88—8—27—32
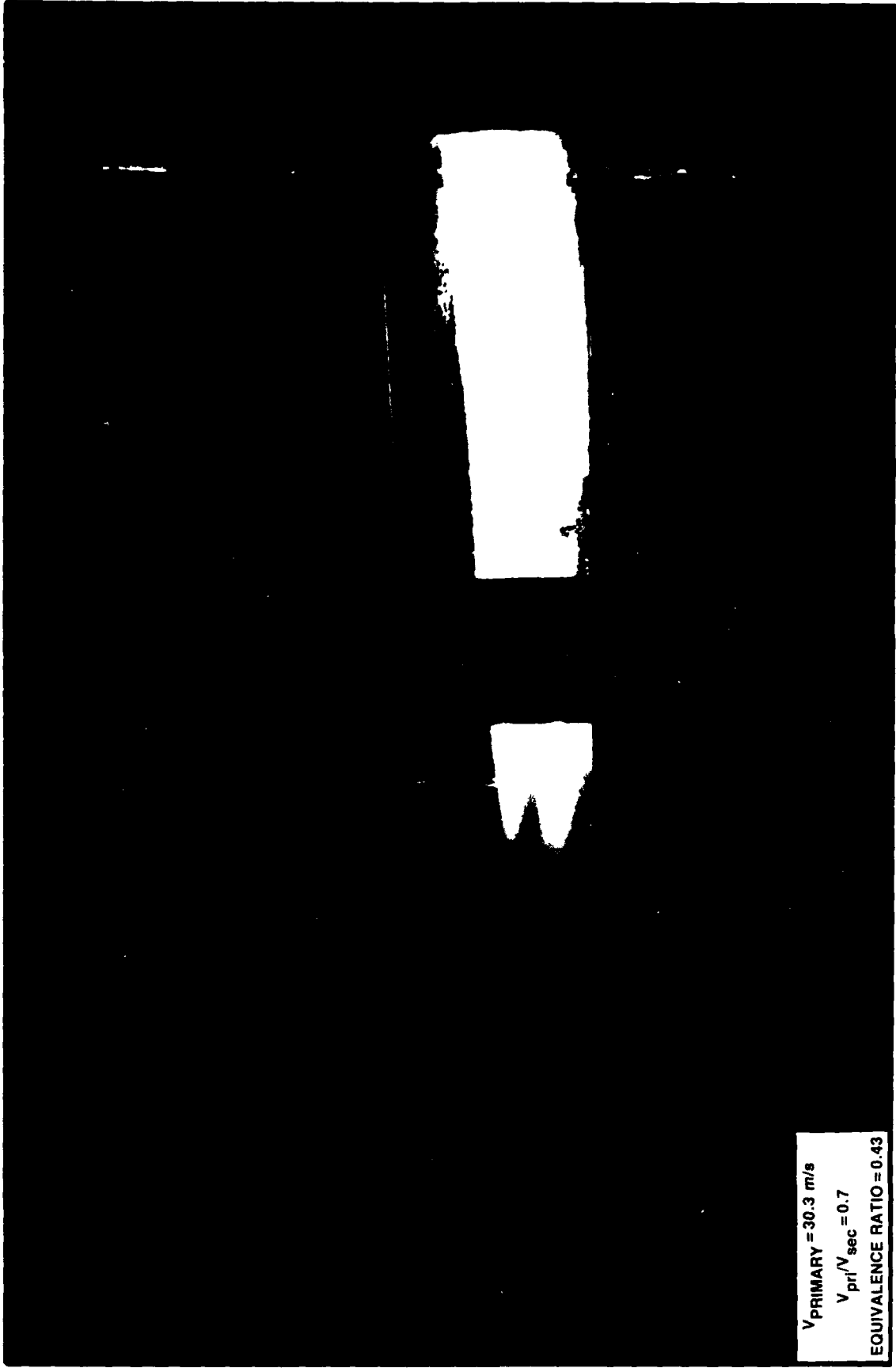
Plate 4.   Flame photograph — flat plate with ramp (test 120).
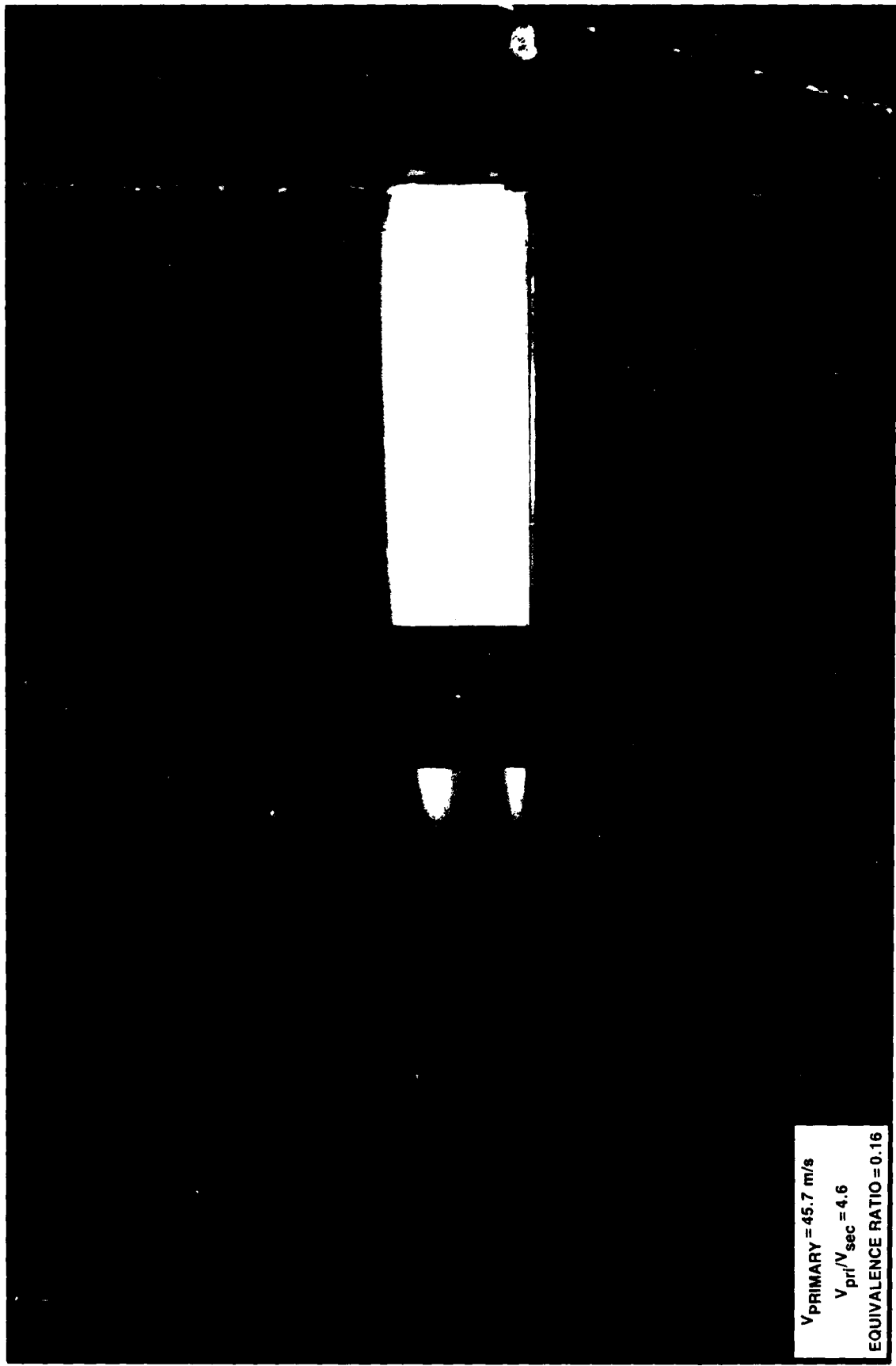
V_PRIMARY = 45.7 m/s
V_{pri}/V_{sec} = 4.6
EQUIVALENCE RATIO = 0.16

Plate 5. Flame photograph — 18% penetration lobe (test 52).

88—8—27—33

$V_{PRIMARY} = 45.7\ m/s$
$V_{pri}/V_{sec} = 4.6$
EQUIVALENCE RATIO = 0.16

88—8—27—34
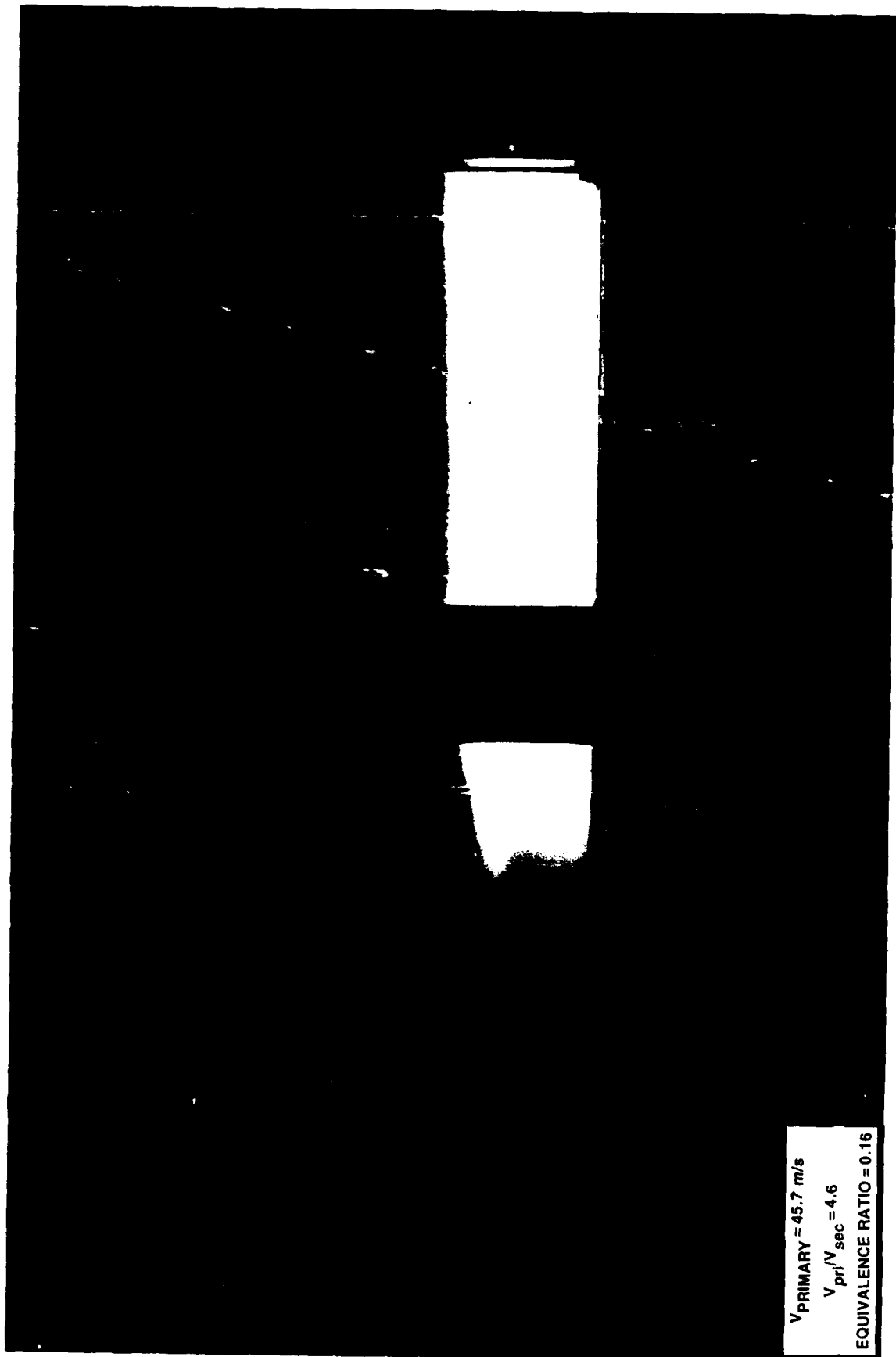
Plate 6.   Flame photograph — 35% penetration lobe (test 56).
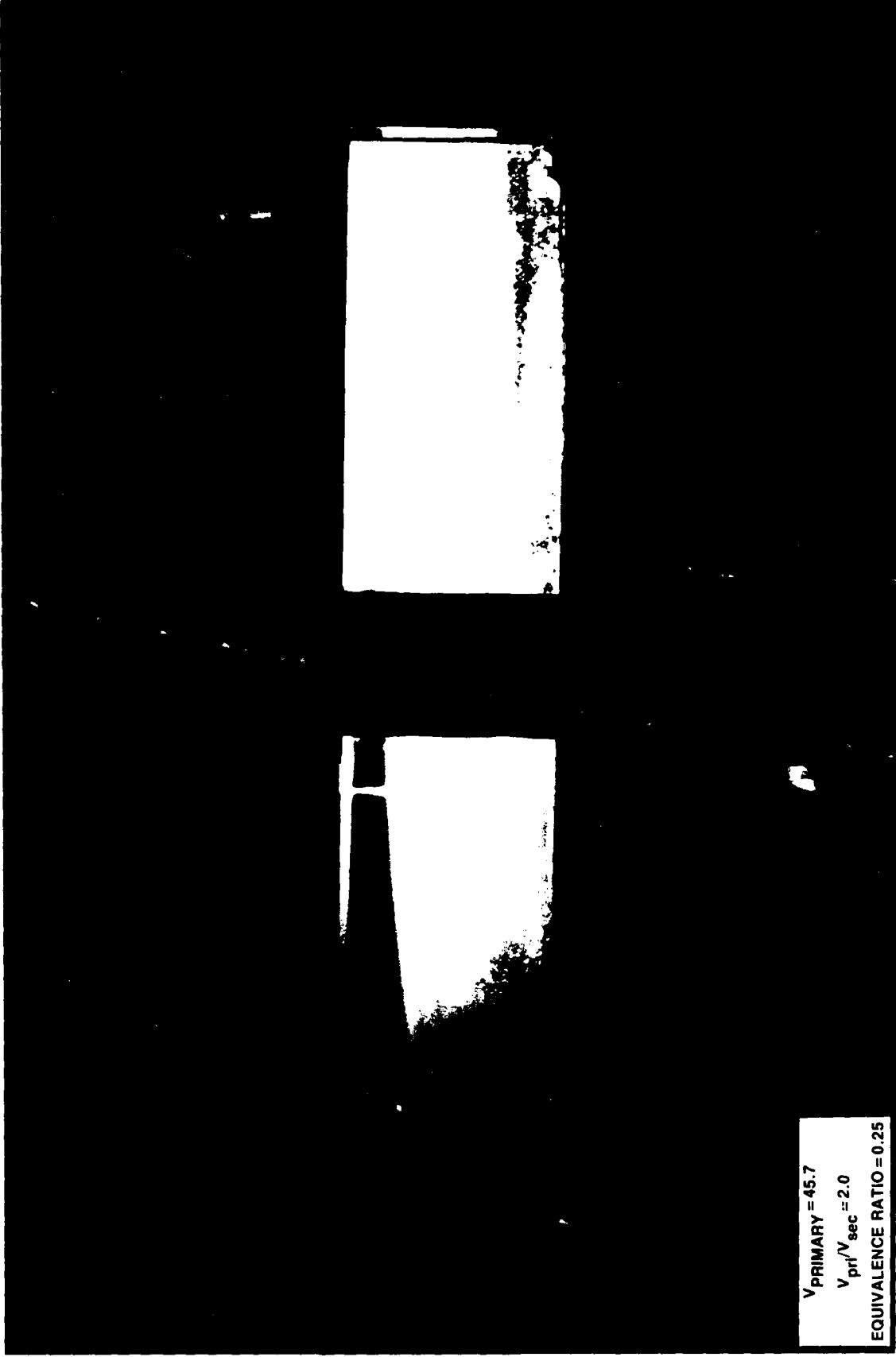
V_{PRIMARY} = 45.7
V_{pri}/V_{sec} = 2.0
EQUIVALENCE RATIO = 0.25

Plate 7.   Flame photograph — 35% penetration lobe with ramp (test 137).

88—8—27—35

APPENDIX I

CHARACTERISTICS OF TRIETHYLBORANE

The physical and chemical characteristics of triethylborane (TEB) as reported by Texas Alkyl, Inc. are given in Table AI.

The equilibrium flame temperature for the combinations of air, nitrogen, and TEB used in this program is shown in Fig. AI. The mass ratios of the constituents are expressed in terms of the ratio of velocities of the air and nitrogen/TEB streams and the TEB air equivalence ratio. The stoichiometric fuel-air ratio for a TEB-air mixture is 0.068.

Triethylborane (TEB)

Formula: $(CH_3CH_2)_3B$

Formula Weight: 98.00

Specifications:

Component	Specification	Typical Analysis
Triethylborane	95 wt% (min)	98 wt%

Physical Properties:

State (at ambient temperatures):	Liquid
Color:	Colorless
Flash Point:	Lower than freezing point
Viscosity:	0.30 centipoise @ 25 C[1]
Density (g/ml):	0.6850 @ 20 C[2], 0.6761 @ 30 C[2]
Freezing Point:	-92.9 C[2,3]

Vapor Pressure:

Temperature (°C)	Vapor Pressure (Torr)		
0	10[3]	12.5[4]	13[5]
20	37[3]		40[5]
40	105[3]		104[5]
60	238[3]		234[5]
80	451[3]		474[5]
95	760[3]		760[5]

Solubility:	TEB is completely miscible with aliphatic and aromatic hydrocarbons, ethers and tertiary amines. It is unreactive and immiscible with water. TEB slowly reacts with alcohols or carboxylic acids to yield ethane and an alkylboron alkoxide or carboxylate.
Stability to Air:	Ignites on exposure (pyrophoric).
Stability to Water:	No reaction.
Storage Stability:	Stable at normal handling temperatures.
Corrosiveness:	Most common metals not attacked.
Surface Tension:	19.84 dynes/cm @ 30 C[5]
Refractive Index:	$n_D^{20} = 1.3971$, $n_D^{30} = 1.3920$[2]
Dielectric Constant:	1.974 @ 20 C, 1.962 @ 30 C[2]
Heat of Combustion (kcal/mole):	$-1,096.9$[1]; $-1,189$[6] (to form crystalline B_2O_3, liquid H_2O and gaseous CO_2)
Heat of Formation (kcal/mole):	(liquid @ 25 C) -47.2 ± 3.7[6] (liquid @ 25 C) -45.4[7], -51.4[7] (gas @ 25 C) -42.6[2]

Other Physical Properties:

|	
Infrared Spectra[8,9,10]	NMR Spectra[11,12]
Quadripole Resonance Spectra[13]	Raman Spectra[14]
Gas Chromatographic Analysis[15,16,18]	Mass Spectra[15,16,17]
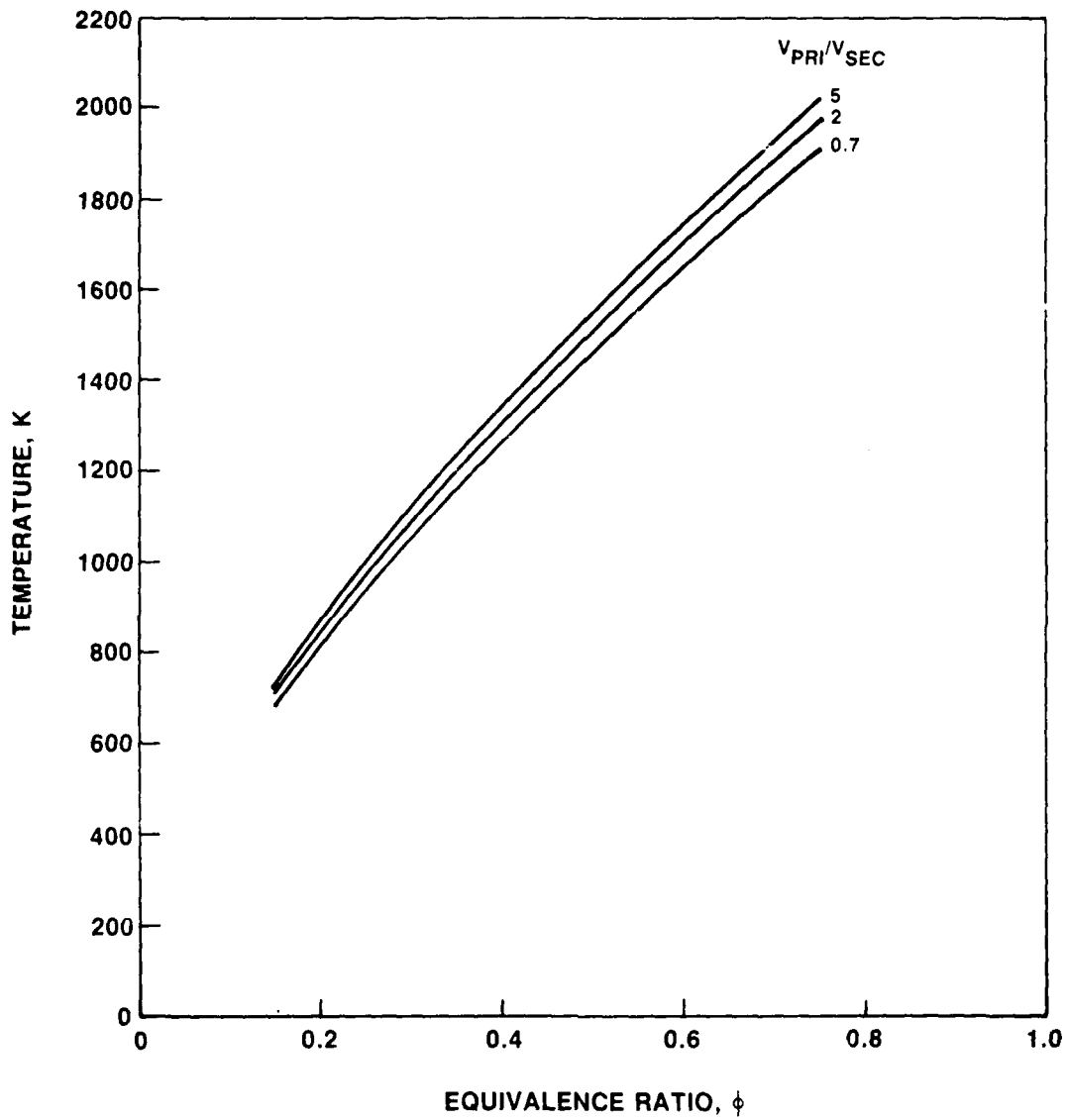
Fig. A.   Equilibrium gas temperature.

APPENDIX II - TEST FACILITY

STREAMWISE-VORTICITY-STIRRED COMBUSTION

The SVS Combustion Test Facility is comprised of three elements: the fuel and air delivery systems, the test apparatus, and the control system.

Delivery Systems

Standard Systems

Air, nitrogen, and fuel are delivered to the test apparatus which is located in an explosion-proof test cell. Flexibility in the gas delivery system is provided by a network of valves and flanged sections; this permits either the airflow or the nitrogen flow to be passed through an electrical heater. A schematic diagram illustrating the capabilities of the flow system and showing a commonly used configuration is given in Fig. AII-1. Two air sources are available; a nominal 27 atm system which can deliver 4.5 kg/sec of air on a continuous basis and larger flow rates on an intermittent basis. It is possible to heat this air using an indirect-fired heater to a temperature of approximately 530 deg K. A second air source can supply unheated air at a nominal pressure of 41 atm at flow rates to 2.3 kg/sec. Gaseous nitrogen is delivered from a 425-cum, 136-atm storage tank. Flow rates on the order of several kg/s are available. Gas flow rates are established by regulated control of the pressure upstream of choked venturis.

A 750 KW electric heater is available to heat either the nitrogen or the air stream. The gases can be heated to temperatures up to 900 K. The flow rate which can be delivered through the heater is pressure dependent; several kg/sec can be delivered at atmospheric pressure. Control of the temperature of the gas delivered to the test apparatus is accomplished manually.

Standard fuel delivery systems available include Jet-A and propane; a special system for the delivery of pyrophoric fuel is also available. Jet-A is delivered at pressures to 100 atm. Flow rates are established by dome-loaded regulator valves; flow rates are monitored by turbine meters. Propane is delivered in liquid form at pressures to 47 atm. Either propane or air was used as the fuel which was delivered to the primary stream when testing in the premixed mode. The fuel is injected far upstream of the preparation section entrance (40 L/D) to provide for vaporization and mixing. The fuel was injected from two spray bars which spanned the duct. Each spray bar was fabricated from 0.635-mm dia stainless steel tubing. Each had two 7-mm dia discharge orifices located 1 cm from the duct axis and oriented such that the fuel was sprayed normal to the airflow direction. The spray bars were oriented normal to one another and were connected to a common manifold. A ball valve permitted flow to one of the two legs to be shut off, such that either a two-orifice or a four-orifice injection mode could be selected.

Whereas these fuel delivery systems are standard, the system used for the delivery and control of the TEB was developed specifically for this facility; the description follows.

Special System - TEB Delivery

Liquid triethylborane is delivered to the test apparatus from the storage cylinder by displacing the TEB with pressurized nitrogen; the maximum pressure is limited by the rated pressure of the cylinders in which the TEB is shipped by the supplier. For this application DOT-4BA low-pressure-gas cylinders having a service pressure of 16 atm were used. The system is capable of delivering flows on the order of several kg/min.

In addition to providing for the delivery of TEB; the system was designed to provide for the purging and the flushing of all delivery lines. Purging was performed using pressurized nitrogen; flushing was accomplished using Jet-A fuel. The purging/flushing operation is required to remove all traces of TEB from the system and thereby preclude ignition of residual fuel when fittings are unsealed during system maintenance or configuration alteration operations. A clean system was required in order to prevent clogging of the fuel injector due to boric oxide formation which will eventually occur when air migrates through the (necessarily unsealed) injector during inactive periods.

A schematic diagram of the system is shown in Fig. AII-2. The major lines designated are:

1) Regulated nitrogen supply
2) Cylinder pressurization (nitrogen)
3) Cylinder relief
4) Jet-A supply
5) TEB delivery

Each line is equipped with gas and liquid check valves; the nitrogen pressurization line was equipped with a relief valve which was set for 10 atm for these tests. The lines are also equipped with solenoid valves which were under control of the microcomputer which was used to select the function to be performed (deliver, purge, etc).

Two features of the system which were included to facilitate operation were the disposal line and the cylinder relief line. The disposal line permits fluids to be discharged into a separate container as opposed to passing through the injector orifice into the test apparatus; bypassing of the small-orifice injector is required to keep the purge and flush times short--on the order of 10 sec. The cleaning procedure used, which is controlled by the microcomputer, is to purge through the injector for 10 sec, then purge through the disposal line, then flush through each line. The procedure is followed at the end of each test day. A second feature was added for safety purposes--the cylinder relief line permitted the TEB cylinder to be depressurized before personnel were admitted to the test cell.

Neither of the two legs of the delivery system which connect directly to the TEB cylinder can be purged in the normal manner. The pressurization line or input to the cylinder is effectively purged by backflow of nitrogen when the storage cylinder pressure is relieved, and therefore accumulation of TEB

is avoided. The delivery line cannot be purged unless the cylinder is emptied. In practice, cylinders were changed without being totally emptied; this requires safety precautions to deal with the combustion of the highly malodorous residual fuel.

All components with which the TEB came in contact were stainless steel; valves were equipped with Kel-F seals. Bellows valves were used to eliminate the possibility of TEB leakage past actuators. The line used were standard 6.35 mm tubing. The instrument used to monitor the flow rate was a Micromotion Mass Flow Meter which senses mass flow by measuring the deflection of a vibrating V-tube--this instrument is completely sealed.

The TEB was delivered to a manifold from which the fuel was injected into the secondary flow stream (nitrogen) at a station 90 L/D upstream of the preparation section entrance. Two Spraying Systems FullJet 1/8GD wall-mounted injectors oriented 90 deg apart on the pipe circumference were employed; a valve permitted the use of either one or two injectors.

Test Apparatus

A general description of the test apparatus was provided in the main body of the report. Additional features are included hereunder.

Both the preparation section and the test section, Fig. 12, were fabricated from commercially available square pipe having a nominal thickness of 0.635 cm. The material is carbon steel. The nominal pressure rating specified at design time was 2 atm. The test apparatus design was selected on the basis of minimization of design and fabrication costs. Accordingly, the dimensions of the sections were dictated by commercially available stock. Also, the location of the preparation section splitter was fixed; joints were continuous, deep penetration welds. Mechanical joints were not used in order to guard against any possibility of the pyrophoric fuel leaking into the oxygen-bearing primary stream.

The function of the preparation section is to deliver reasonably uniform flows to the surface of the splitter plate. The primary stream was delivered by a 40 L/D length of pipe to the flanged entrance to the preparation section. A perforated plate (20% open area, 0.2 cm dia holes) was sandwiched between the flanges to provide flow straightening. The flow to the secondary stream entered the undersurface of the preparation section; a bundle of 15-cm long, 0.635-mm dia tubes within the preparation section served as a flow straightener in this stream. During rig qualification testing, pitot pressure traverses were conducted to insure that the mass flux distributions were reasonably uniform. No efforts were undertaken to document boundary layer thicknesses or turbulence levels.

A flanged section joins the preparation and combustion sections. The splitter surface protrudes from the preparation section such that various splitter trailing edge designs can be joined to form the desired splitter configuration. A sketch showing the method of joining is given along with other details in Fig. AII-3. No special provisions were made for sealing

either this joint or the line of contact between the splitter plate edge and the wall of the combustion section. Post-test examination of the test hardware did not indicate the presence of any thermal distress resulting from leakage of the reactants in this region. Further, there was no evidence of any mechanical vibration of the cantilevered lobe support.

The combustion section was lined with 3.8 cm. thick Fiberfrax Duraboard which is a rigid material fabricated from alumina and silica fibers. No active cooling was employed. The panels originally installed in the test section were employed throughout the test effort with no maintenance required. The only evidence of distress was some slight erosion. The cross-section view in Fig. AII-3 illustrates the installation.

The test section was equipped with windows fabricated from fused quartz. Commercial grade quartz of 2.54 cm thickness was employed. The material was specified to be suitable for photographic purposes; the optical quality far exceeded the requirements given the difficulty of maintaining clean surfaces in the presence of boric oxide formation. The construction of the window frames used to retain the windows is also shown in Fig. AII-3.

Control System

A general description of the control system was provided in the main body of the report where it was noted that a combination of manual and microcomputer-based controls were used. A description of the computer-based operation is provided below.

The function of the computer-based system was to ensure that the sequence of operations involving the TEB system was performed in an orderly manner. Uncontrolled delivery of TEB to the wrong environment constituted a fire hazard which was to be avoided by a system of interlocks and controls.

An Apple IIe computer provided the necessary speed, memory capacity, and flexibility for this application. The computer was equipped with ADALAB laboratory interfacing equipment which supplied multi-channel A/D conversion capability as well as digital output for the activation of relays. A screen display of the state of all functions was provided; floppy disks were used to store recorded data.

A schematic diagram of the control system is given in Fig. AIII-4; the dashed lines illustrate the sensor connections which were as follows:

o Thermocouples, labeled TN2 and TAIR sensed the temperature of the gas streams in the preparation section. If a failure or crack occurred which permitted the streams to mix, combustion would be initiated which could destroy the uncooled preparation section. Therefore, fuel flow was not permitted unless TN2 and TAIR were lower than a selectable limit.

o Pressure transducer PN2 sensed the pressure upstream of the choked venturi which controlled the flow of nitrogen. TEB was not permitted to be delivered to the nitrogen stream unless the venturi pressure exceeded a prescribed level.

o Pressure transducer PAIR sensed the pressure upstream of the choked venturi which monitored the flow of air. TEB was not permitted to be delivered unless the air venturi pressure exceeded a prescribed level. Quench water could back flow into the apparatus without a sufficient air momentum; therefore quench water flow was not permitted unless the air venturi pressure was acceptable.

o Pressure transducer PH2O sensed the quench water manifold pressure; fuel was not permitted to flow unless the water pressure exceeded a specified level.

As the test program progressed, it became apparent that the integrity of the system was satisfactory and that damage from preignition in the preparation section was unlikely. Therefore the thermocouples TAIR and TN2 were relocated to the combustion section where their output was used to sense the existence of flame. In this location, the thermocouples were designated T1 and T2, the temperatures were recorded as a function of the time from run start and the data recorded on disk to be made available for analysis.

LEGEND

⧓ SHUT-OFF VALVE

⧗ CHECK VALVE

⧓⌐ REGULATOR VALVE

⧗ RELIEF VALVE

)(VENTURI

◖ BURST DISK

2000 psi NITROGEN SYSTEM

600 psi AIR SUPPLY

400 psi AIR SUPPLY

N_2 2 in.

3 in.

HEATER

FILTER

SECONDARY FUEL

PRIMARY FUEL

SVS COMBUSTION TEST APPARATUS

EXHAUST
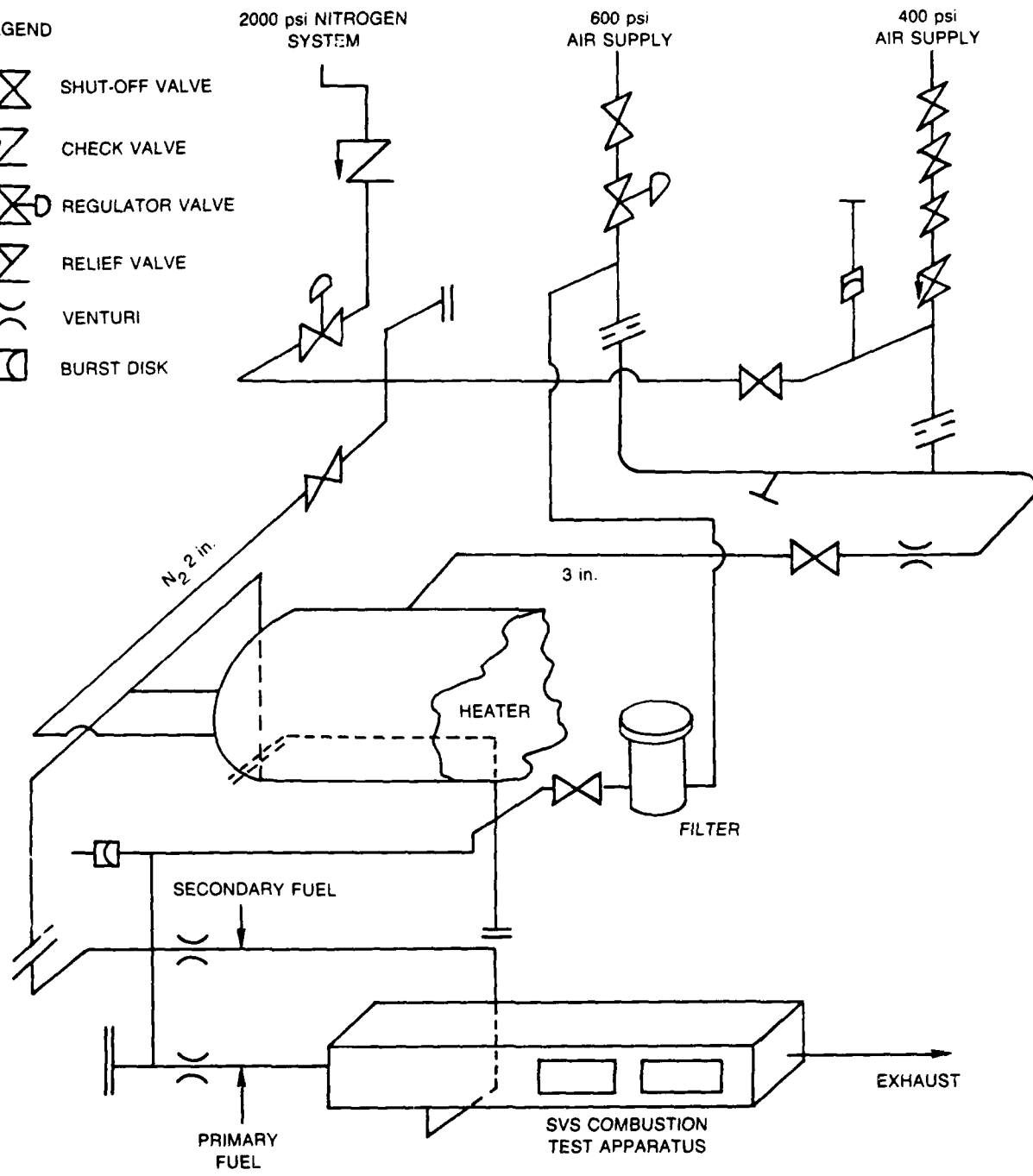
Fig. AII-1   SVS combustion facility flow diagram.

88—6—83—7

Fig. AII – 2 TEB delivery system.

LEGEND

⊗	SOLENOID VALVE		
	PRESSURE TRANSDUCER		
	MASS FLOW METER		
	FILTER		
(T)	THERMOCOUPLE		
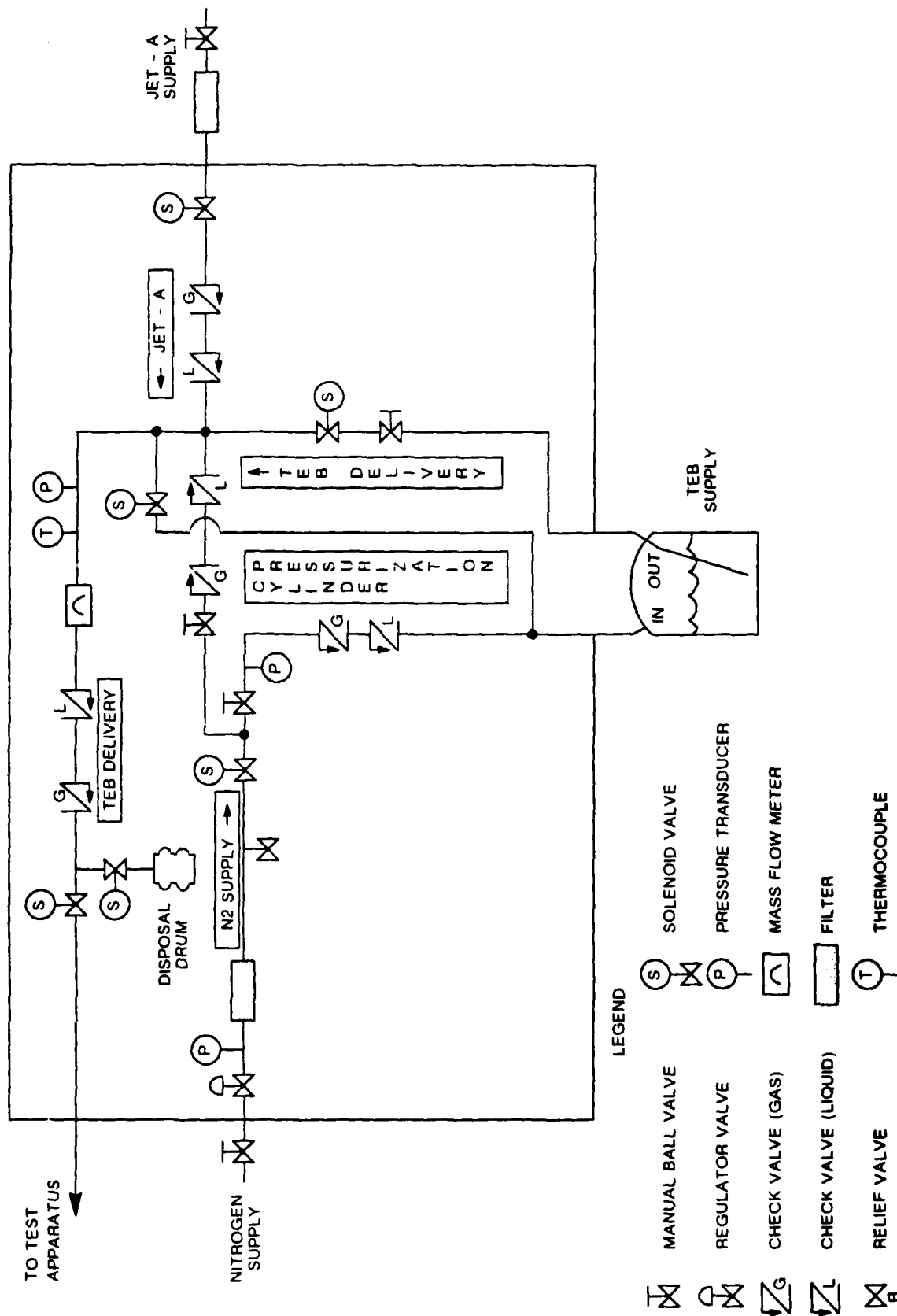
⋈ MANUAL BALL VALVE

⋈ REGULATOR VALVE

⋈ᴳ CHECK VALVE (GAS)

⋈ᴸ CHECK VALVE (LIQUID)

⋈ᴿ RELIEF VALVE

88-8-27-19

CONVOLUTED SPLITTER

RAMP

PREPARATION SECTION ← → TEST SECTION
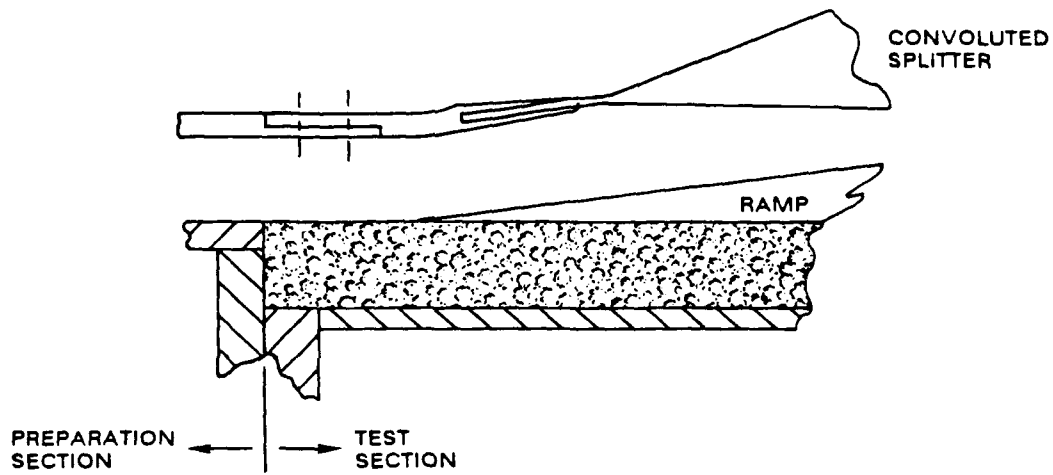
LOBED SPLITTER ATTACHMENT SCHEME

11.7

1.68

PREPARATION SECTION
CROSS-SECTION

14 cm

QUARTZ WINDOW

CERAMIC

14 cm

CERAMIC CEMENT

BOLT

BOLT

TEST SECTION
DETAILS
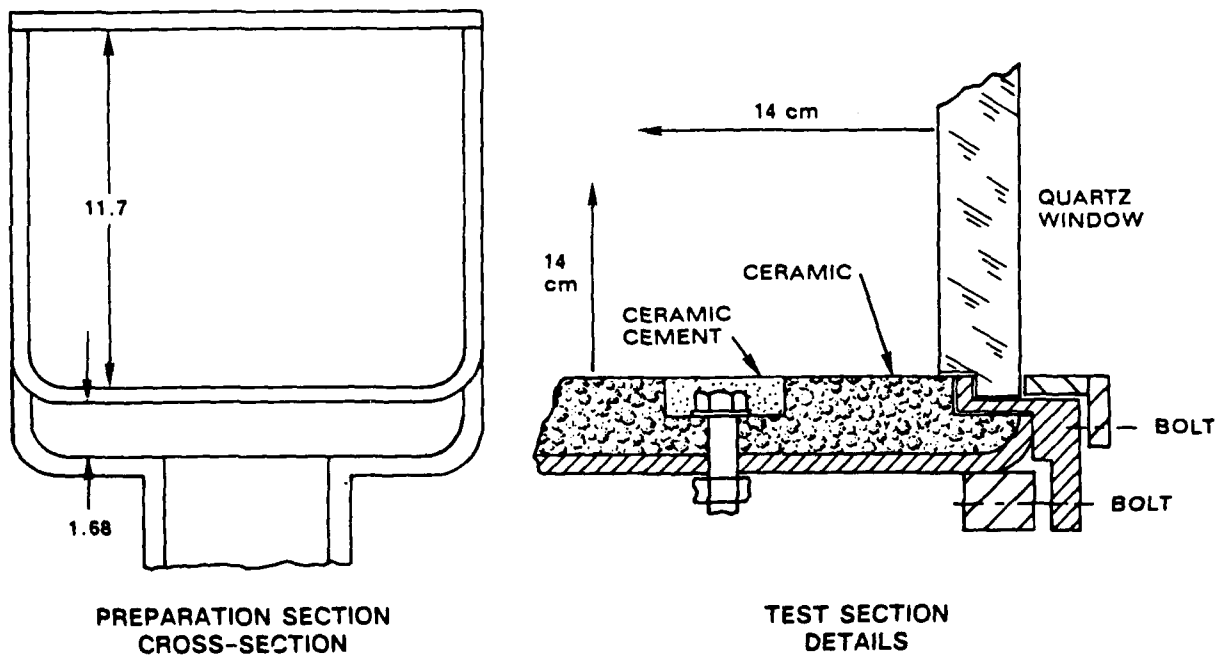
Fig. AII – 3   Test apparatus details.

88-8-27-20

Fig. AII-4 SVS combustion facility control system.

EXHAUST

P_{H_2O}

QUENCH
WATER
SUPPLY

R_2

TEBN_2 NITROGEN AIR
CONTROL ROOM GAUGES

R1
R6
R7

TEB
SYSTEM

NITROGEN SUPPLY

T_{AIR}
T_{N_2}
R_4

C_3H_8

R_5

NITROGEN
SUPPLY

P_{N_2}

TEB
N_2

N_2

HAND LOADERS

P_{AIR}

AIR

R_3

FUEL
SUPPLY

AIR

APPLE IIE
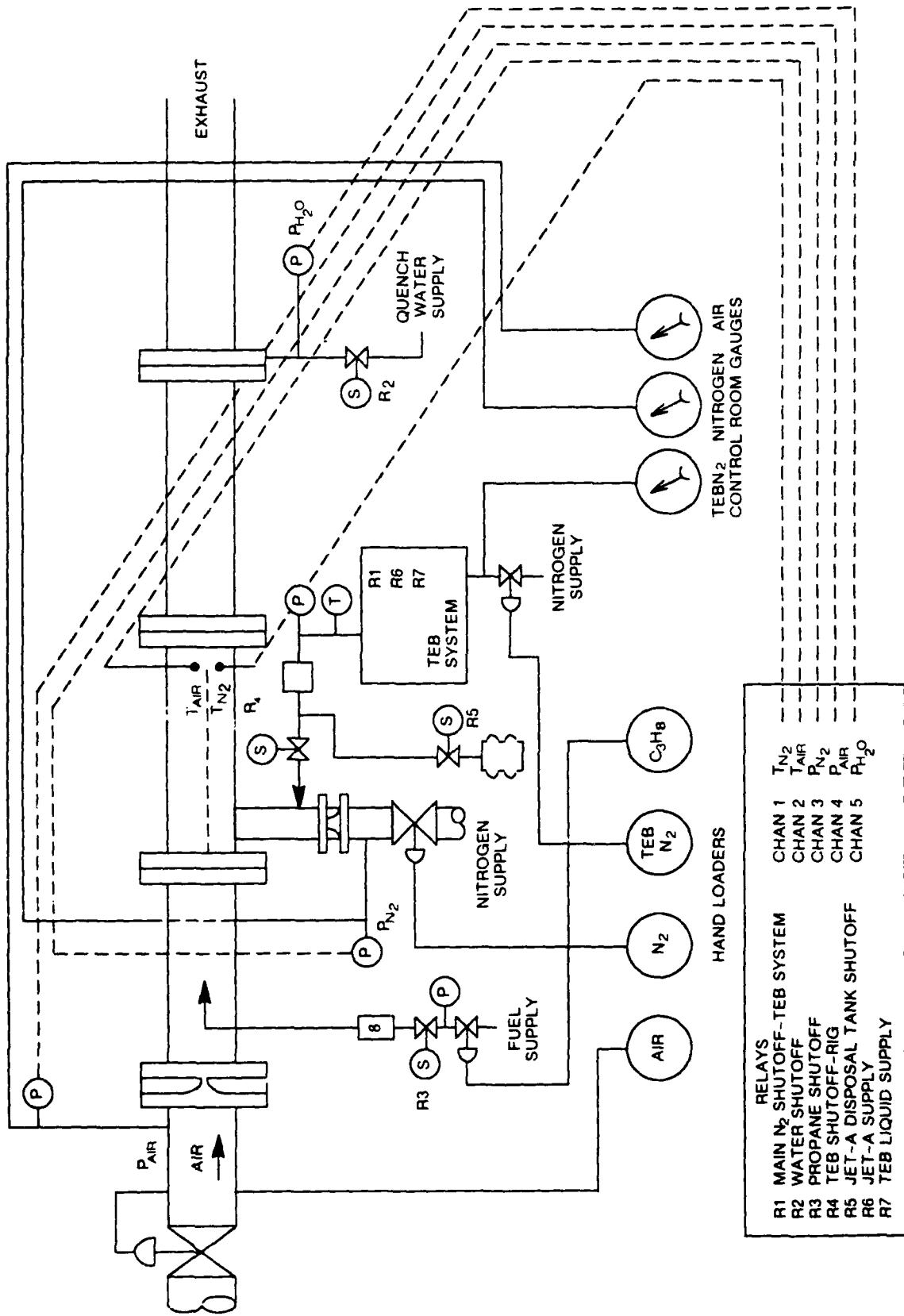
RELAYS
R1 MAIN N_2 SHUTOFF–TEB SYSTEM
R2 WATER SHUTOFF
R3 PROPANE SHUTOFF
R4 TEB SHUTOFF-RIG
R5 JET-A DISPOSAL TANK SHUTOFF
R6 JET-A SUPPLY
R7 TEB LIQUID SUPPLY

CHAN 1 T_{N_2}
CHAN 2 T_{AIR}
CHAN 3 P_{N_2}
CHAN 4 P_{AIR}
CHAN 5 P_{H_2O}

88-8-27-21

APPENDIX III - FAST RESPONSE PRESSURE TRANSDUCER

An "ultra-miniature" silicon diaphragm transducer having an operating range from 0 to 1.7 atm (25 psi) with a sensitivity of approximately 47 mv per atm was used to obtain information on the pressure fluctuations which developed during combustion. The transducer used was similar in characteristics to the Model EPI-6B-255 unit produced by Entran Devices, Inc. The transducer was mounted in an instrumentation port located on the top of the test section at a station approximately 53 cm downstream of the trailing edge of the splitter plate. The active sensing element was located at the end of a 25.4 mm long x 2.7 mm diameter cavity. An acoustic response calculation showed that the lowest resonant frequency of the cavity is 3350 Hz at ambient conditions and the response is flat to within three percent for frequencies up to 500 Hz. The transducer was calibrated over the operating range and found to be linear to within six percent of full scale.

The data were recorded using the facility data acquisition system (JETDAS) which utilizes a Perkin Elmer 3205 computer. The data rate selected was 1000 Hz with transducer output above 500 Hz being surpressed by signal conditioning. The gain level was elected such that the maximum signal accepted without saturation was 0.14 atm (2 psi). Because of the low signal relative to the transducer range, signal drift was encountered. This drift was compensated for at test time by adjusting the signal conditioner zero level at run time. The data acquisition time was 4.096 sec. Only a single channel of data was collected. Checks showed that the variation in sampling time associated with operating the acquisition system in this mode was negligible.

The data were analyzed using the PE3205-based SPAG Signal Processing software published by Cranfield Data Systems. All data in the 4096 record block were analyzed. No filtering or other manipulation of the data was employed. The data analysis system was used to generate the time spectrum of the transducer output so that the amplitude and dominant frequencies of the combustion chamber oscillations could be identified.

## APPENDIX IV – DIGITIZED FLAME ENVELOPES

FLAT PLATE TEST 37

PRIMARY VELOCITY = 45.72 m/sec SECONDARY VELOCITY = 9.91 m/sec TEB FLOW RATE = 0.59 kg/min
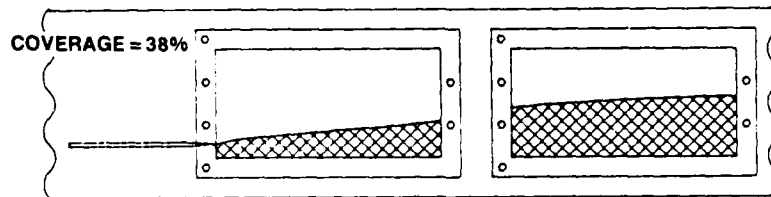
COVERAGE = 38%

FLAT PLATE TEST 49

PRIMARY VELOCITY = 45.72 m/sec SECONDARY VELOCITY = 9.91 m/sec TEB FLOW RATE = 0.59 kg/min

COVERAGE = 46%
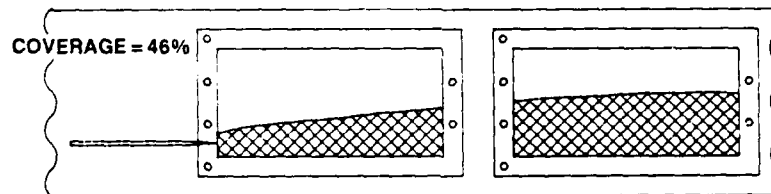
FLAT PLATE TEST 103

PRIMARY VELOCITY = 45.72 m/sec SECONDARY VELOCITY = 45.72 m/sec TEB FLOW RATE = 1.1 kg/min

COVERAGE = 40%
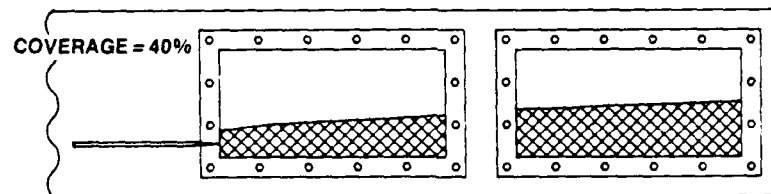
FLAT PLATE TEST 104

PRIMARY VELOCITY = 38.1 m/sec SECONDARY VELOCITY = 45.72 m/sec TEB FLOW RATE = 1.04 kg/min

COVERAGE = 42%
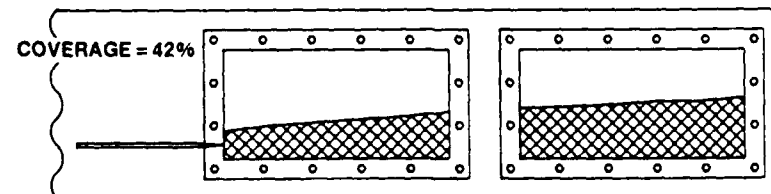
Fig. AIV-1   Flame envelope — flat plate.

88—8—27—24

FLAT PLATE WITH RAMP TEST 120

PRIMARY VELOCITY = 30.48 m/sec SECONDARY VELOCITY = 45.72 m/sec TEB FLOW RATE = 1.04 kg/min

COVERAGE = 52%
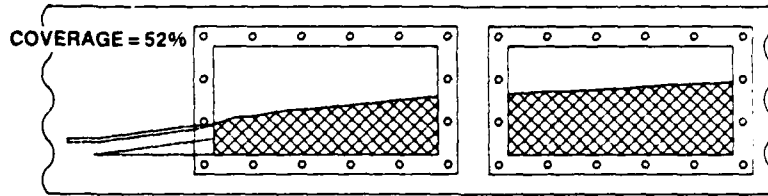
FLAT PLATE WITH RAMP TEST 123

PRIMARY VELOCITY = 45.72 m/sec SECONDARY VELOCITY = 15.24 m/sec TEB FLOW RATE = 1.09 kg/min

COVERAGE = 54%
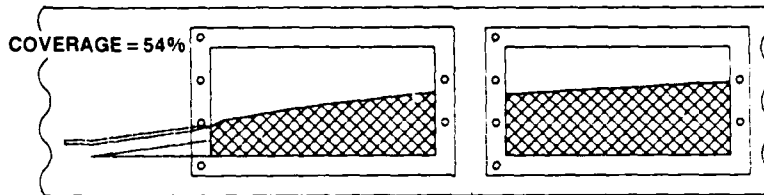
FLAT PLATE WITH RAMP TEST 125

PRIMARY VELOCITY = 45.72 m/sec SECONDARY VELOCITY = 30.48 m/sec TEB FLOW RATE = 0.99 kg/min

COVERAGE = 51%
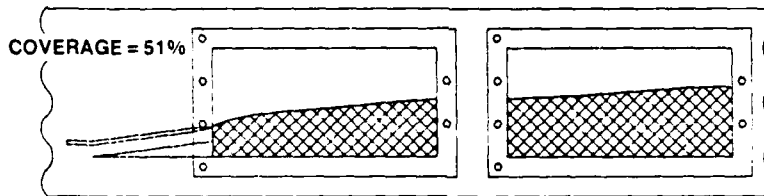
FLAT PLATE WITH RAMP TEST 128

PRIMARY VELOCITY = 60.96 m/sec SECONDARY VELOCITY = 30.48 m/sec TEB FLOW RATE = 1.13 kg/min

COVERAGE = 51%
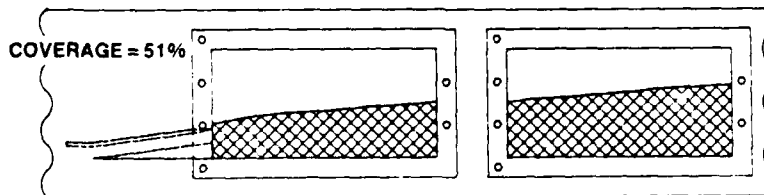
Fig.. AIV-2   Flame envelope — flat plate with a ramp.

88—8—27—25

18% PENETRATION LOBE TEST 52

PRIMARY VELOCITY = 45.72 m/sec SECONDARY VELOCITY = 9.91 m/sec TEB FLOW RATE = 0.59 kg/min

COVERAGE = 59%
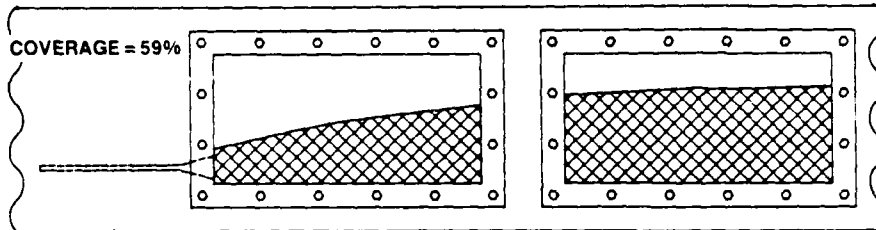
18% PENETRATION LOBE TEST 53

PRIMARY VELOCITY = 45.72 m/sec SECONDARY VELOCITY = 15.24 m/sec TEB FLOW RATE = 0.61 kg/min


COVERAGE = 60%
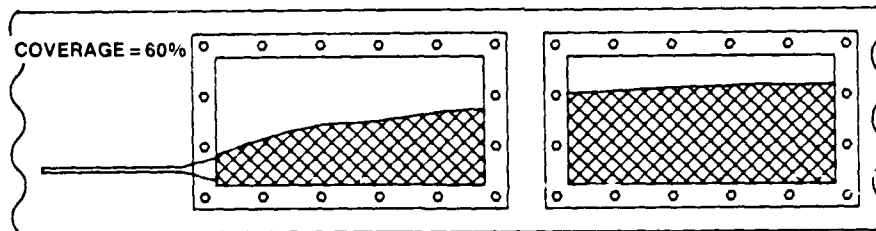
18% PENETRATION LOBE TEST 55

PRIMARY VELOCITY = 45.72 m/sec SECONDARY VELOCITY = 22.86 m/sec TEB FLOW RATE = 0.59 kg/min

COVERAGE = 59%
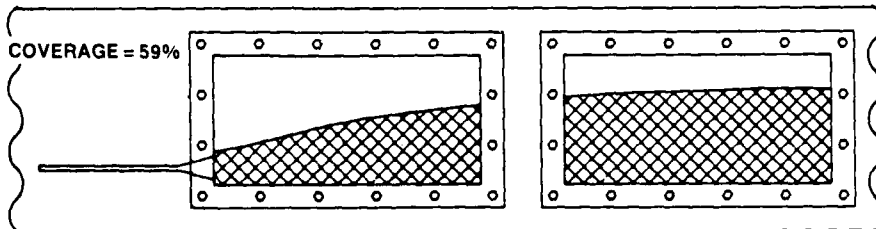
Fig. AIV-3   Flame envelope — 18% penetration lobe.

88—8—27—26

35% PENETRATION LOBE TEST 56

PRIMARY VELOCITY = 45.72 m/sec SECONDARY VELOCITY = 9.91 m/sec TEB FLOW RATE = 0.59 kg/min

COVERAGE = 62%
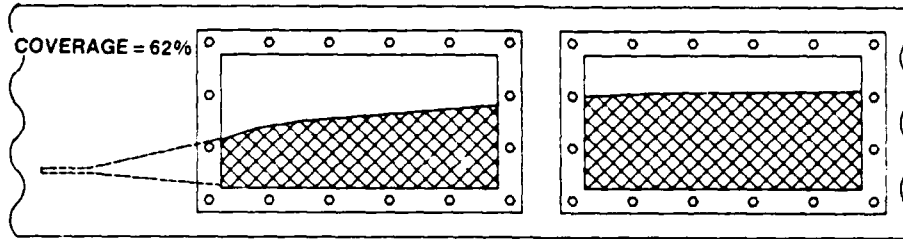
35% PENETRATION LOBE TEST 62

PRIMARY VELOCITY = 45.72 m/sec SECONDARY VELOCITY = 9.91 m/sec TEB FLOW RATE = 0.5 kg/min

COVERAGE = 69%
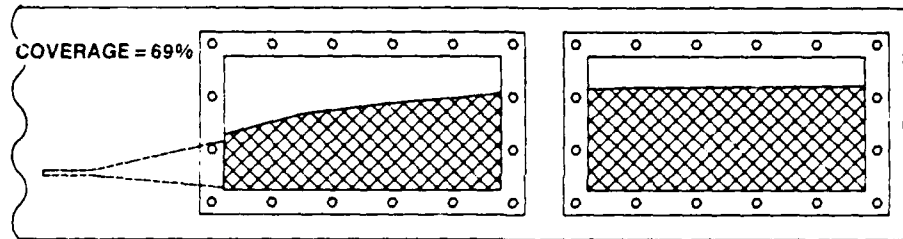
35% PENETRATION LOBE TEST 61

PRIMARY VELOCITY = 45.72 m/sec SECONDARY VELOCITY = 11.28 m/sec TEB FLOW RATE = 0.59 kg/min

COVERAGE = 65%
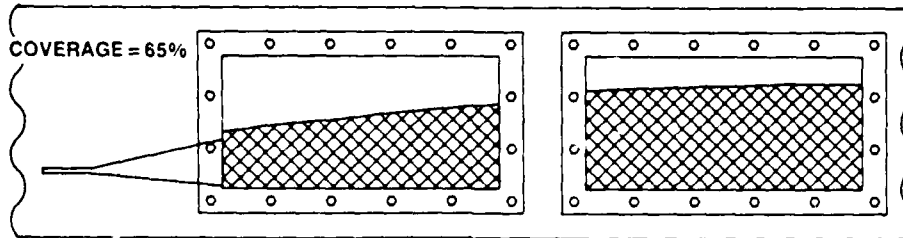
Fig. AIV-4   Flame envelope — 35% penetration lobe.

35% PENETRATION LOBE WITH RAMP TEST 88

PRIMARY VELOCITY = 26.82 m/sec SECONDARY VELOCITY = 22.86 m/sec TEB FLOW RATE = 0.66 kg/min

COVERAGE = 90%
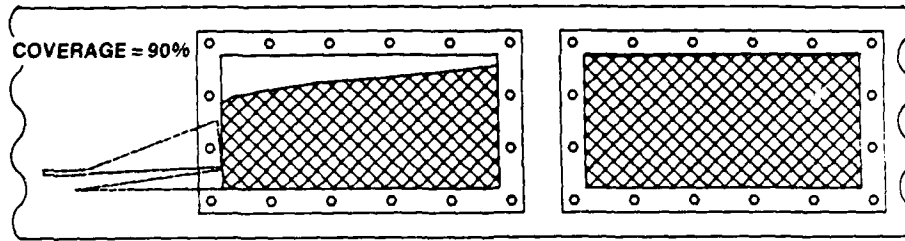
35% PENETRATION LOBE WITH RAMP TEST 91

PRIMARY VELOCITY = 38.1 m/sec SECONDARY VELOCITY = 45.72 m/sec TEB FLOW RATE = 1.09 kg/min

COVERAGE = 90%
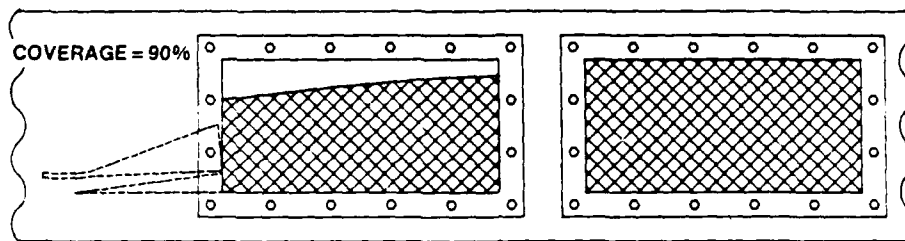
35% PENETRATION LOBE WITH RAMP TEST 136

PRIMARY VELOCITY = 200 m/sec SECONDARY VELOCITY = 100 m/sec TEB FLOW RATE = 2.2 kg/min

COVERAGE = 78%
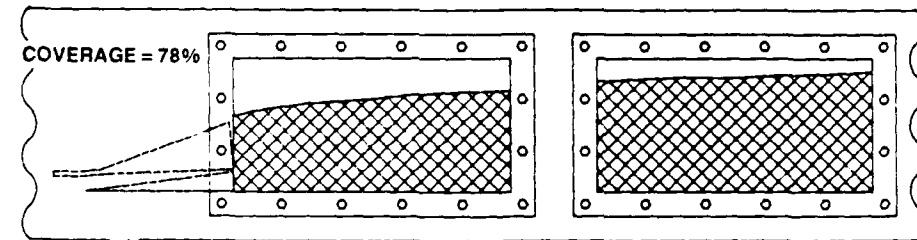
35% PENETRATION LOBE WITH RAMP TEST 137

PRIMARY VELOCITY = 45.72 SECONDARY VELOCITY = 6.1 m/sec TEB FLOW RATE = 0.92 kg/min

COVERAGE = 64%
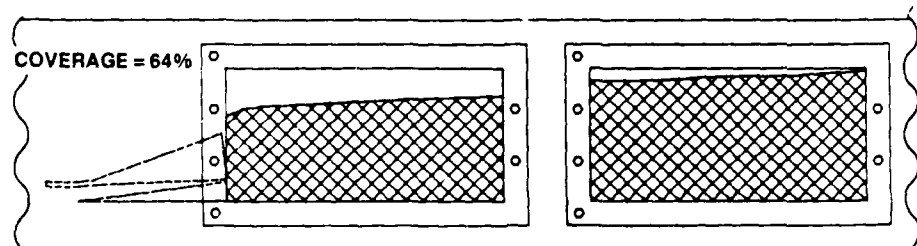
Fig. AIV-5   Flame envelope — 35% penetration lobe with ramp.

88—8—27—27